

Table2Charts: Learning Shared Representations for Recommending Charts on Multi-dimensional Data *

Mengyu Zhou, Qingtao Li, Yuejiang Li, Xinyi He, Yibo Liu, Shi Han, Dongmei Zhang

Microsoft Research
Beijing, China

{mezho, v-qingtl, v-yuejli, v-hexin, v-yiboliu, shihan, dongmeiz}@microsoft.com

Abstract

It is common for people to create different types of charts to explore a multi-dimensional dataset (table). However, to build a real-world intelligent assistant that recommends commonly composed charts, it should take the challenges of efficiency, imbalanced data hungry and table context into consideration. In this paper, we propose Table2Charts framework which learns common patterns from a large corpus of (table, charts) pairs. Based on deep Q-learning with copying mechanism and heuristic searching, Table2Charts does table-to-sequence generation, where each sequence follows a chart template. On a large spreadsheet corpus with 167k tables and 271k charts, we show that Table2Charts could learn a shared representation of table fields so that tasks on different chart types could mutually enhance each other. Table2Charts outperforms other chart recommendation systems in both multi-type task (with almost doubled recall numbers $R@3=0.62$ and $R@1=0.44$) and human evaluations.

1 Introduction

Creating charts for a multi-dimensional dataset (denoted as table) is a common activity in many domains like sales, human resources, investment, engineering, scientific research, education, *etc.* To perform routine analysis and discover insights, people spend a huge amount of time constructing different types of charts (such as the ones in Figure 1) to present diverse perspectives on their tables. This tedious process often requires experience and expertise in data analytics and visualization to create proper charts. It is important to build intelligent assistants in a data-driven way to generalize common wisdom on chart composing for general users.

To help chart designers in the real world, the following two recommendation tasks are essential for charting assistant tools: **single-type** task which recommends a specific type of charts for a given table, and **multi-type** task where a ranked list of multiple common types of charts are recommended together. When facing a table for the first time, one usually has no clear idea about what chart analysis should be created. In this scenario, an assistant could help exploit past common wisdom of what commonly composed charts could be created for the table – which is the multi-type task. Then a user may want to explore diverse (and even minor) types of charts for inspirations – which is the single-type task. Later

with a clearer intention in mind, the main obstacle for the user is the efforts needed to realize ideas through complex charting UIs. Since most tools (such as Excel) put chart type buttons / choices as the top entry points to chart composing, guessing and suggesting auto-filling and completion of the details of a chosen chart type – which is the single-type task – could help save time and efforts from users.

A long line of works tried to make chart creation easier by recommending **data queries** (selecting *what* data to analyze) and/or **design choices** (*how* to visualize selected data), such as DeepEye (Luo et al. 2018), Data2Vis (Dibia and Demiralp 2019), DracoLearn (Moritz et al. 2019) and VizML (Hu et al. 2019). However, most of them did not address the single-type task and some of them did not recommend data queries. There are still lots to improve on the performance and efficiency of chart recommendation systems.

When tackling the single-type and multi-type tasks with both data queries and design choices, there are three fundamental challenges. First, **separate costs**: It is memory and speed inefficient to design, train and deploy models for multi-type task and single-type tasks repeatedly and independently. Second, **imbalanced data hungry**: The available data for different chart types are highly imbalanced. Four major types of charts cover 98.91% of the available charts while others rarely appear because it is hard for non-experts to create them. Lack of data in minor chart types makes it hard to build high-quality models for them. Third, **table as context**: Selecting and visualizing data from a table depend on not only the data statistics, but also the semantic meanings of the whole table context. Proper models need to be designed to take table context into chart recommendation.

In this paper, we propose **Table2Charts** framework for learning and recommending commonly composed charts for each given table. In §2, charts recommendation is formulated as table to sequence(s) problem with next-action-token estimation to fill chart template(s). Then in §3, as the estimation heuristic for customized beam searching, we design an encoder-decoder deep Q-value network (DQN) which selects table fields to fill a template via copying mechanism. All recommendation task shares one encoder but has their own decoders, which addresses the separate costs challenge. The DQN is trained using mixed learning on the multi-type task of major chart types. By exposing its encoder part to the diverse source tables of different chart types, it learns **shared**

*Preprint. Under review.

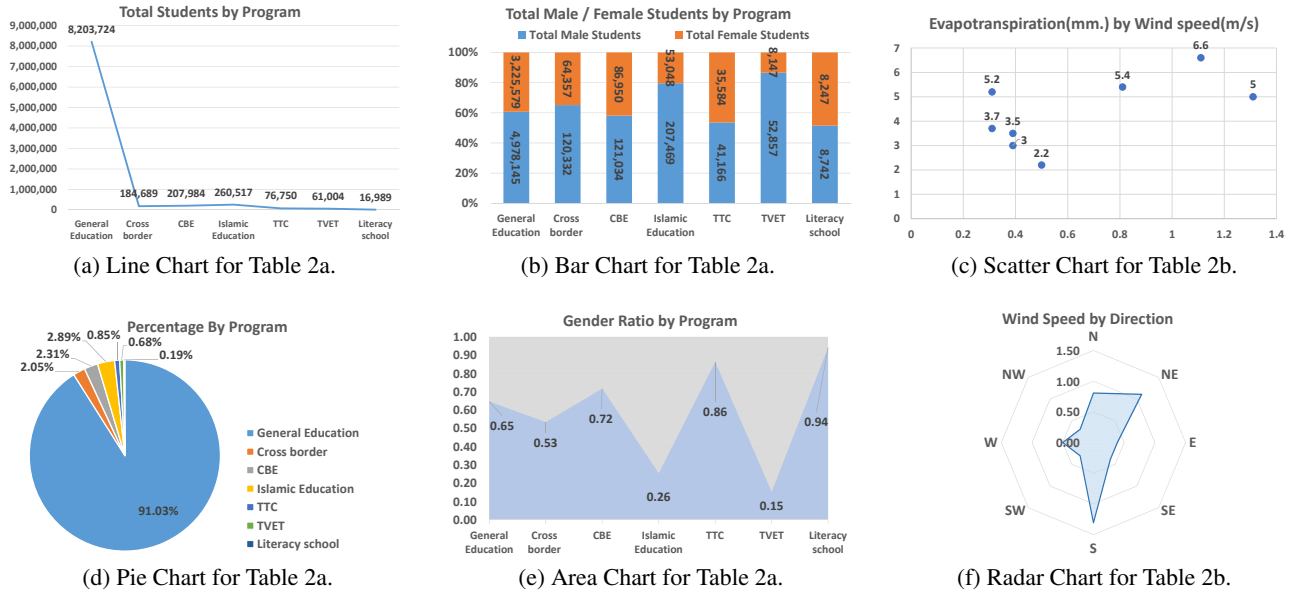


Figure 1: Example Charts for Tables in Figure 2.

table representations containing semantic and statistic information of table fields. Then this pre-trained table representation is transferred for type-specific decoders of single-type tasks, relieving the imbalanced data problem.

From the public web, we collect a large corpus of 271250 charts created from 167329 tables and use public dataset – Plotly to verify the effectiveness of Table2Charts framework in §4. For each chart type, the recall for top-3 and top-1 recommendations are 60.4% – 93.8% and 50.8% – 80.7% on single-type task. The multi-type task of recommending major chart types has 61.7% recall at top-3 and 44.4% recall at top-1, which exceed the baseline methods by 36.6% on average. Human evaluation are also conducted to validate the performance of the proposed framework. Through visualization, we find that the DQN could learn shared table representations during multi-type task training for later transfer learning, thus improving the performance and saving memory occupation of single-type tasks. These experiments justify that Table2Charts could efficiently learn the common wisdom of creating charts.

In summary, our main contributions are:

- Table2Charts framework is proposed by us to learn human chart composing wisdom. It generates both data queries and design choices in an action sequence for multi-type and single-type chart recommendation tasks with the state of the art performance and efficiency.
- To the best of our knowledge, we conduct the largest scale (167k tables and 271k charts) training with diverse evaluations (two large corpora) of chart recommend systems.
- We show the feasibility of learning shared table representations (encoding table fields into embedding vectors) for enhancing down-stream data analysis tasks.

2 Problem

For a given table with multiple data fields, what meaningful charts could be created? We formulate this problem as building machine learning models that learn patterns from large amounts of (table, charts) pairs, and generates commonly composed charts for a given table.

A table here is an n -dimensional dataset \mathcal{D} which contains n data fields $\mathcal{F}_{\mathcal{D}} = (f_1^{\mathcal{D}}, \dots, f_n^{\mathcal{D}})$. Each data field refers to an attribute of the dataset with its corresponding header name (attribute metadata) and data values (records). For example, each column from tables in Figure 2 is a data field with its first row as header.

To demonstrate our ideas, as shown in Figure 1, in this paper we pick four major and two minor chart types (see appendix §A for more details) commonly appeared in charting tools such as Excel. The major types are line, bar, scatter and pie charts. The minor types are area and radar charts.

All these charts have common creation process of referencing data fields for its x and y axes. In this section, we unify the action space (actions to create charts) and define templates for different chart types. Then, both single-type and multi-type chart recommendation tasks can be formulated as the problem of table to action sequences.

2.1 Chart Templates

Although different types of charts exhibit distinct visual effects and behaviors, the essential actions for creating them from table can be summarized into two types: Selecting / referencing table fields and running specific charting commands / operations to organize and plot the selected fields. In this sense, a chart can be regarded as a sequence of actions on data queries and design choices. To describe the grammar for each chart type, we define the possible actions and constraints on them as below.

Program	Total Male Students	Total Female Students	Gender Ratio	Total Male Students Percentage	Total Female Students Percentage	Total Students	Total Program Students Percentage
General Education	4,978,145	3,225,579	0.65	60.68%	39.32%	8,203,724	91.03%
Cross border	120,332	64,357	0.53	65.15%	34.85%	184,689	2.05%
CBE	121,034	86,950	0.72	58.19%	41.81%	207,984	2.31%
Islamic Education	207,469	53,048	0.26	79.64%	20.36%	260,517	2.89%
TTC	41,166	35,584	0.86	53.64%	46.36%	76,750	0.85%
TVET	52,857	8,147	0.15	86.65%	13.35%	61,004	0.68%
Literacy school	8,742	8,247	0.94	51.46%	48.54%	16,989	0.19%

(a) Student Statistics Table.

Date	Evapotranspiration (mm.)	Dir.	Wind speed (m/s)
1-May-2010	5.4	N	0.81
19-May-2010	6.6	NE	1.11
6-Jul-2010	3.0	E	0.39
3-Aug-2010	3.5	SE	0.39
1-Sep-2010	5.0	S	1.31
12-Sep-2010	3.7	SW	0.31
23-Sep-2010	2.2	W	0.50
14-Oct-2010	5.2	NW	0.31

(b) Evapotranspiration and Wind Table.

Figure 2: Two Example Tables.

Definition 1 (Action Space / Tokens). For an n -dimensional table \mathcal{D} , there are two types of action tokens $\mathcal{A}_{\mathcal{D}} = \mathcal{F}_{\mathcal{D}} \cup \mathcal{C}$ representing core actions of composing a chart:

- *Field referencing token* $f \in \mathcal{F}_{\mathcal{D}}$ that indicates a field is selected for composing chart.
- *Command tokens* (denoted as \mathcal{C}) which defines other commands for structuring a chart, including:
 1. Chart type tokens, such as [Line] means to start composing a line chart sequence;
 2. Separator [SEP] which splits the referenced fields with different roles in a chart sequence;
 3. Group operations in $\mathcal{G} = \{[\text{Cluster}], [\text{Stack}]\}^1$ indicating how to put multiple data values from multiple fields (series) together along the x axis.

Then we can define how to represent different types of charts using the unified action tokens. Different from language modelling in NLP, here action tokens should be organized into a sequence according to specific grammar rules / hard constraints of a chart type. The rules could be written as the following templates.

Definition 2 (Chart Grammar Templates). The template of each major and minor chart type (see appendix §A for more details) can be defined in the Backus-Naur form as follow:

$$\begin{aligned}
\langle \text{Line} \rangle & \models [\text{Line}] \langle f+ \rangle [\text{SEP}] \langle f^* \rangle [\text{SEP}] \\
\langle \text{Bar} \rangle & \models [\text{Bar}] \langle f+ \rangle [\text{SEP}] \langle f^* \rangle \langle \text{grp} \rangle \\
\langle \text{Scatter} \rangle & \models [\text{Scatter}] \langle f \rangle [\text{SEP}] \langle f \rangle [\text{SEP}] \\
\langle \text{Pie} \rangle & \models [\text{Pie}] \langle f \rangle [\text{SEP}] \langle f^* \rangle [\text{SEP}] \\
\langle \text{Area} \rangle & \models [\text{Area}] \langle f+ \rangle [\text{SEP}] \langle f^* \rangle [\text{SEP}] \\
\langle \text{Radar} \rangle & \models [\text{Radar}] \langle f+ \rangle [\text{SEP}] \langle f^* \rangle [\text{SEP}]
\end{aligned}$$

where $\langle \text{grp} \rangle$, $\langle f^* \rangle$, $\langle f+ \rangle$ and $\langle f \rangle$ are placeholders: $\langle \text{grp} \rangle \models$ an operation $\in \mathcal{G}$, $\langle f^* \rangle \models \lambda \mid \langle f \rangle \langle f^* \rangle$, $\langle f+ \rangle \models \langle f \rangle \mid \langle f \rangle \langle f+ \rangle$, and $\langle f \rangle \models a \text{ field} \in \mathcal{F}_{\mathcal{D}}$, λ means empty. The first $\langle f+ \rangle$ or $\langle f \rangle$ segment means the field(s) mapped to y-axis as value series, while the second $\langle f^* \rangle$ segment is the field(s) mapped to x-axis. (Multiple fields can be concatenated for x-axis.)

¹ [Cluster] means the values from several fields are put side-by-side, while [Stack] means accumulating them one-upon-another for each x category / label (E.g., Figure 1b).

For example, from the table in Figure 2a, two charts Figure 1a and 1b are created. Their action sequences are [Line] (Total Students) [SEP] (Program) [SEP], and [Bar] (Total Male Students) (Total Female Students) [SEP] (Program) [Stack], respectively.

Note that how x and y axes behave depends on chart type: E.g., scatter and pie charts only have one value series; temporal records will be sorted along x-axis on a line chart; etc.

Also, other types of hard constraints are included in the template definitions to restrict heuristic beam searching (see next section). E.g., the data type of a field mapping to y-axis is forbidden to be string type.

In this paper, we only focus on the core parts of data queries and design choices – How to select and compose fields as axes of proper chart type. There are more charting aesthetics (Wilke 2019) to consider, such as shape, size, color, line width and type, etc. Meanwhile, for the sake of simplicity, we only deal with database-like tables and referencing a whole field without filtering, aggregation, bucketing or ordering. These are more subtle aspects to an analysis and could also be incorporated into chart sequences in the future. The semantic structure of a spreadsheet table (Dong et al. 2019a) could provide useful information when selecting data. This could also lead to interesting future work.

2.2 Table to Sequence Generation

With the above definitions, now the task of chart recommendation becomes filling the placeholders of template(s), in other words, generating action token sequences that follow the grammars of the given template(s). Note that the first chart type token of single-type task is fixed, and the generation starts from the second token, while multi-type sequence generation task starts from the first chart type token.

One way to fill the template is to generate a sequence one token by another from left to right. The differences between generating an NL sequence and a chart sequence are: 1) Chart sequence should follow the strict grammar defined by the corresponding template, while in NL there are no strict rules written down as templates; 2) In NLP the vocabulary (the token set) is usually fixed and indexed, while in charts, for each unique table \mathcal{D} its action space $\mathcal{A}_{\mathcal{D}}$ differs from action spaces of other tables on field referencing tokens.

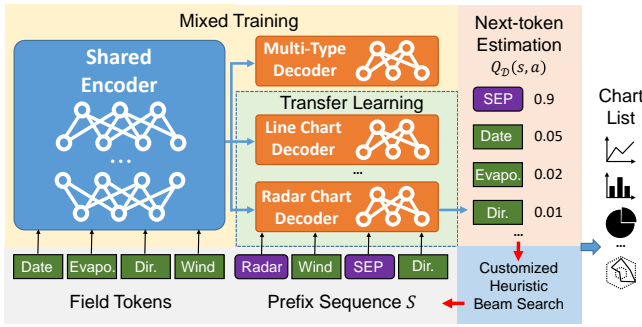


Figure 3: Overview of Table2Charts Framework.

Given a table \mathcal{D} and an incomplete chart sequence s , we can define the valid actions space of the sequence as $\mathcal{A}_{\mathcal{D}}(s)$ according to its corresponding template. A common way to solve sequence generation problem is to learn an estimation function for heuristic beam searching (see appendix §D.4). Follow the language modelling formulation in (Zhou et al. 2020), we choose $Q(s, a) = \mathcal{P}(sa \in \mathcal{T}_{\mathcal{D}}^+ | s, \mathcal{D})$ as action-value function to guide the choice of action token $a \in \mathcal{A}_{\mathcal{D}}(s)$. Here $\mathcal{T}_{\mathcal{D}}^+$ is the set of all target chart sequences (the charts that would be adopted by user for \mathcal{D}) and their prefixes. So the optimal action-value function $q_*(s, a) = \begin{cases} 1 & \text{if } s' = sa \text{ and } s' \in \mathcal{T}_{\mathcal{D}}^+, \\ 0 & \text{otherwise.} \end{cases}$ is the learn-

ing target for $Q(s, a)$. (More details of the corresponding Markov decision process can be found in appendix §D.1.) In §3 we will discuss how to approximate $q_*(s, a)$ by deep Q-Network (DQN) with copying mechanism.

3 Method

In Table2Charts we design an encoder-decoder DQN architecture with copying mechanism to fill chart templates. Since the exposure bias is severe for sequence generation with templates, we adopt search sampling technique to train while beam searching. Finally, in order to solve the imbalanced data problem and mutually enhance the performance among different chart types, in Table2Charts we first mix the major chart types to train together to get a mixed model. The mixed encoder part is a shared table representation that will be transferred to each single-type task for decoder tuning. The mixed encoder-decoder is also used directly for the multi-type task. The whole pipeline of Table2Charts is shown in Figure 3. The details and implementation code can be found in appendix §D.

3.1 Filling Templates: DQN with Copying

As shown in Figure 4, we design a DQN (deep Q-network) $Q(s, \mathcal{A}_{\mathcal{D}})$ to approximate $q_*(s, a)$. $Q(s, \mathcal{A}_{\mathcal{D}})$ takes all the fields $\mathcal{F}_{\mathcal{D}} = (f_1, \dots, f_n)$ and a state $s = s_0 \dots s_{T-1}$ as its input, and calculates the estimated action values ($\in [0, 1]$) for all $a \in \mathcal{A}_{\mathcal{D}}$. Only the output for $\mathcal{A}_{\mathcal{D}}(s)$, i.e. the valid actions *w.r.t.* the template grammar of s , are considered.

In Figure 4a is our customized CopyNet architecture (details in appendix §D.2). There are several differences be-

tween our model and the original CopyNet encoder-decoder architecture (Gu et al. 2016): First, unlike the typical CopyNet condition in NLP where vocabulary size is far greater than the length of the copying source, vocabulary (the command tokens) in Table2Charts is pretty small while the universe of table fields is infinite, and there is no overlapping between generate mode (for vocabulary) and copy mode (for table fields). Second, similar to the approach in (Zhou et al. 2020), the input tokens to $Q(s, \mathcal{A}_{\mathcal{D}})$ first go through a feature transformation network in Figure 4b $e(\cdot)$ rather than the usual index to embedding matrix in normal NLP. The feature transformation network aggregates different kinds of information of a field: the semantic embedding calculated from header name using pre-trained models like FastText (Bojanowski et al. 2017) or BERT (Devlin et al. 2018), a variety of categorical features (e.g., string / numerical / temporal, is currency, etc.), and a diverse set of statistics calculated from record values. In appendix §D.3 we further describe the feature details. Third, the output of $Q(s, \mathcal{A}_{\mathcal{D}})$ is a vector of $[0, 1]$ values for each action, rather than a probability distribution over the action space in the original CopyNet.

Our design of DQN with copying mechanism is naturally suited for the tasks to generate structures from table fields. It handles the open vocabulary of table field universe and provides a clear division between table representation (encoder) and template filling (decoder). The encoder part will take in the whole **table context** and generate field embedding vectors. As good $q_*(s, a)$ estimator, $Q(s, \mathcal{A}_{\mathcal{D}})$ is then used by Table2Charts as a heuristic function in beam searching to generate multiple sequences.

3.2 Fixing Exposure Bias: Search Sampling

The typical way to train a next-token estimator is through teacher forcing (Williams and Zipser 1989) by only sampling the prefix sequences of user-created chart analyses, and comparing the estimated actions with actual user actions. In other words, the samples used to train $Q(s, \mathcal{A}_{\mathcal{D}})$ network come from a corpus of (table, analysis) pairs following the format of Equation (2.2) with $s \in \mathcal{T}_{\mathcal{D}}^+$.

As discussed in (Ranzato et al. 2016; Zhou et al. 2020), with only teacher forcing, the outcome model could face exposure bias problem which is common in sequence generation. During teacher forcing, the model is only exposed to the ground truth states (target prefixes) while at inference it has only access to its own predictions. As a result, during generation it can potentially deviate quite far from the actual sequence to be generated, leading to a biased estimation.

To mitigate exposure bias, we take the search sampling approach in (Zhou et al. 2020) to close the gap between training and inference. Inspired by reinforcement learning, the search sampling process adopts $Q(s, \mathcal{A}_{\mathcal{D}})$ as the heuristic function to conduct beam searching on each table (see appendix §D.4). Then the expanded states (including s not in $\mathcal{T}_{\mathcal{D}}^+$) will be stored in a replay memory for periodical update of $Q(s, \mathcal{A}_{\mathcal{D}})$ itself. This process is very effective after the warm-up of the network with teacher forcing. Without search sampling, the model would perform poorly (can lead to unacceptable performance in §4.2), especially with the customized beam searching process limited by templates.

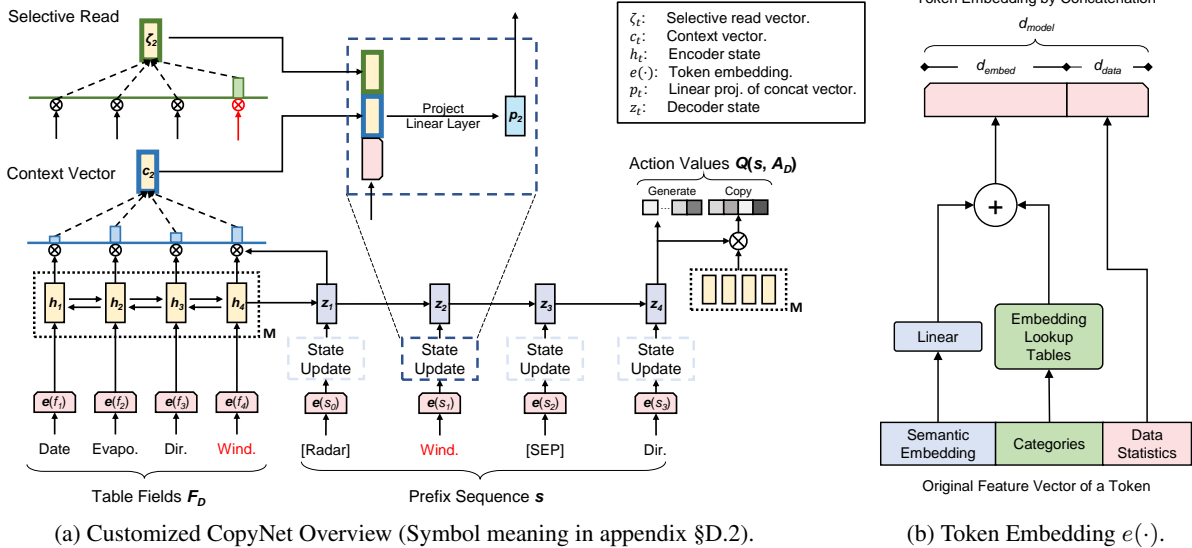


Figure 4: $q_*(s, a)$ Approximator: DQN Model Architecture.

3.3 Mixed Training and Transfer Learning

The DQN designed in §3.1 has the encoder-decoder architecture, where encoder computes table fields’ representation embeddings, and decoder consumes the provided representations for sequence generation. As shown in Figure 3, our basic idea is that the table representation encoder can be shared by several (one multi-type and six single-type) tasks. This expose the encoder to diverse and abundant table field samples, and reduce the memory occupation and inference time for deploying models of the tasks.

To learn shared table representation encoder and get task-specific decoders, we propose a *mix-and-transfer* paradigm containing two stages: 1) **Mixed Training**: Mixing all major chart types together and train one DQN model. Its mixed encoder will be transferred to the next stage, while the whole mixed DQN will be used for the multi-type recommendation task. 2) **Transfer Learning**: Take the mixed encoder from the previous stage and freeze its parameters. Then, for each single-type task, a new decoder part is trained with the fixed shared encoder using only the data of the chart type.

Comparing to **Separate Training** where a whole DQN is trained for each single-type task using only the data of that chart type, the mix-and-transfer paradigm in Table2Charts has the following advantages: 1) Better memory occupation and inference speed, because now DQN models for all tasks share one same encoder, while separate training still inefficiently holds one for each task. This solves the **separate cost** problem; 2) The encoder is exposed to far more samples than each individual chart type can provide; this not only leads to better learning and generalization of the table representation (see §4.5 to see how **table context** is represented), but also solves the **imbalanced data hungry** problem so that only decoder part (which is small comparing to the larger encoder part) needs tuning for minor chart types.

4 Experiments

In this section, first we introduce the (table, charts) corpus which is used for evaluating Table2Charts. Then the performance of mix-and-transfer paradigm (see §3.3) will be evaluated for both single and multi-type tasks. The experiments are run on Linux machines with 24 CPUs, 448 GB memory and 4 NVIDIA Tesla V100 16G-memory GPUs. We run all experiments for three times and by default all evaluation metrics reported in this section are averaged over three results. Each training consists of 10 epochs of teacher forcing followed by 10 epochs of search sampling (see §3.2).

4.1 Chart Corpora

Our chart corpus contains 113390 (42.59%) line, 67600 (25.39%) bar, 64934 (24.39%) scatter, 17436 (6.55%) pie, 1990 (0.75%) area and 902 (0.34%) radar charts. They are extracted using OpenXML (Microsoft 2018) and TableSense (Dong et al. 2019b) libraries from the spreadsheet files crawled from the public web. After filtering out duplicated tables, extremely large tables (> 128 fields), empty charts and over-complicated charts (with > 4 fields for y-axis), and down-sampling the tables of each table schema (consisting of field names and types of a table), 271250 charts are remained in 167329 unique tables with 99879 different schemas. The schemas (with their tables and charts) are allocated for training, validation and testing in the ratio of 7:1:2.

We also adopt the public Plotly community feed corpus (Hu et al. 2019) and sample 36888 tables with 67617 charts from it for testing in §4.2. It contains 22644 line charts, 20053 scatter charts, 24204 bar charts and 716 pie charts. Details of statistics and processing of Excel and Plotly corpora can be found in appendix §B and §C.

Table 1: Evaluations of Table2Charts and Baseline Methods on Datasets of Different Tasks. (Averaged over 3 runs.)

Dataset	Task	Recall	DeepEye	Data2Vis	Table2Charts
Excel	Data Queries	R@1	34.34%	30.84%	65.14%
		R@3	47.13%	41.53%	77.92%
	Design Choices	R@1	17.84%	17.89%	57.43%
		R@3	20.35%	32.40%	76.66%
	Overall	R@1	10.18%	13.05%	44.43%
		R@3	15.85%	26.82%	61.72%
Plotly	Data Queries	R@1	49.53%	68.53%	83.96%
		R@3	66.37%	73.93%	92.03%
	Design Choices	R@1	38.56%	9.70%	38.97%
		R@3	38.57%	33.55%	55.75%
	Overall	R@1	24.57%	11.26%	34.38%
		R@3	36.43%	24.39%	48.51%

4.2 Evaluations on Multi-Type Reco Task

As mentioned in §3.3, a mixed DQN is first trained using samples of Excel major chart types. Then, the mixed-trained DQN is used as beam searching heuristic function to generate a ranked list of four major types of charts for each table.

Three tasks – data queries, design choices and overall chart recommendation – are evaluated on Excel and Plotly corpora. For data queries we examine whether the recommended fields are used for composing charts by users. For design choices, we evaluate whether models can recommend correct chart type, field mapping and bar grouping operation given the selected fields. For overall chart recommendation, both data queries and design choices are compared with ground truth. Recall at top- k ($k = 1, 3$; R@1, R@3) are adopted as the evaluation metrics. It shows how a ranked list of charts matches the selected fields and user-created charts.

We also compare Table2Charts framework with DeepEye (Luo et al. 2018), Data2Vis (Dibia and Demiralp 2019). Table2Charts and Data2Vis are trained with Excel corpus from scratch, while the public DeepEye model is directly used for evaluation. The comparison experiment setup can be found in appendix §E. The results are shown in Table 1.

From Table 1, we can see that Table2Charts outperforms other baseline methods for all three tasks on both Excel and Plotly dataset. The R@1 and R@3 have reached 44.43% and 61.72% on Excel (34.38% and 48.51% on Plotly), which exceeds those of baseline methods by about 31% (10% on Plotly). This shows that our framework can give good chart analyses recommendations for a table. The data queries numbers are higher on Plotly than those on Excel. This is because Plotly tables only contain fields which are used for composing charts, and thus lower the difficulty of data queries task. The recall of design choices is a bit larger than data queries for Table2Charts framework.

In addition, Table2Charts only takes 9.40ms to make recommendation for a table on average, while it costs DeepEye and Data2Vis 48.19ms and 210ms, respectively. This further shows the practicability and efficiency of Table2Charts.

Human Evaluation is also conducted on another 80 common HTML tables crawled from the public web (see appendix §E.5). The top-1 recommended charts from DeepEye, Data2Vis and Table2Charts are compared for each ta-

Table 2: Evaluations of Three Training Methods on Six Single-Type Tasks. (Averaged over 3 runs.)

	Type(s)	Recall	Separate	Mixed	Transfer
Major Type	Line	R@1	53.98%	53.22%	53.69%
		R@3	69.16%	68.69%	69.75%
	Bar	R@1	59.60%	60.17%	61.01%
		R@3	72.35%	72.57%	73.25%
	Scatter	R@1	56.16%	56.33%	57.13%
		R@3	73.69%	73.30%	74.29%
Minor Type	Pie	R@1	77.51%	78.95%	80.70%
		R@3	92.90%	93.47%	93.81%
	Area	R@1	36.19%	–	50.80%
		R@3	47.77%	–	60.43%
	Radar	R@1	52.34%	–	74.77%
		R@3	67.29%	–	78.50%

ble by 5 experts with more than 4 years of experience in data analysis and visualization. Each recommended chart are rated with an integer score from 1 to 5 (higher score means better chart). We conduct Wilcoxon signed-rank tests (Wilcoxon, Katti, and Wilcox 1970) at 95% confidence level and compute Cliff’s delta effect sizes (Macbeth, Razu-miejczyk, and Ledesma 2010) (details can be found in appendix §E.5). First, comparing Table2Charts with DeepEye, the p-values of Wilcoxon test is less than 0.001 and the Cliff’s delta effect sizes is 0.671 (large). As for the comparison between Table2Charts and Data2Vis, the p-values of Wilcoxon test is 0.05 and the Cliff’s delta effect sizes is 0.201 (small but not negligible). These results show that the recommended charts from Table2Charts are better.

4.3 Evaluations on Single-Type Reco Tasks

After mixed training, as discussed in §3.3, the shared table representation encoder is taken and frozen for the training of six decoders for six single-type tasks. For comparison, the separate training (see §3.3) will generate an independent DQN model for each chart type with the same settings as the transfer learning. The mixed DQN from §4.2 is also directly tested on single-type tasks of major chart types.

The evaluation results are shown in Table 2. In general, the mix-and-transfer paradigm (“Transfer”) works better than separate training (“Separate”) and mixed-only (“Mixed”) model for all chart types. This verifies Table2Charts could also handle single-type tasks well. For line, bar and scatter charts, the recall values of “Separate” are also fairly high compared to “Mixed”. This is because these types of charts have sufficient data for training, and other types of charts, which may add noises to a major type, are excluded from separate training. Considering the model size where the encoder and decoder parts are designed with 1.3M and 0.5M parameters, “Separate” have 10.8M parameters while “Transfer” only has 4.3M. Thus, mix-and-transfer paradigm of Table2Charts is a good choice *w.r.t.* both performance and efficiency (avoiding **separate costs**).

As for minor chart types, there are huge gaps between the performance of “Transfer” and “Separate” in Table 2. As discussed in §1, imbalanced data hungry is the bottleneck of the recommendation for these minor chart types. With

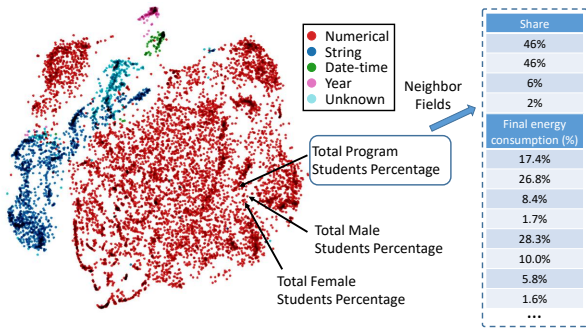


Figure 5: Visualization of Shared Table Representations.

mix-and-transfer paradigm, on average R@1 and R@3 increase 18.5% and 11.9%. The main reason is that the shared encoder could capture and extract the information of table context and field semantics, and the quantity of minor type charts are sufficient to train decoder which is of smaller size. Thus, the **imbalanced data hungry** problem is overcome.

4.4 Recommendation Case Studies

We conduct empirical study of the recommended results on the table in Figure 2a which originally has Figure 1a, 1b and 1e composed by user. When a user does not know where to start, the multi-type mixed model recommends common types of charts. Its top-3 recommendations are:

- (1) [Bar](Total Male Students)(Total Female Students)[SEP](Program)[Stack]
- (2) [Bar](Total Male Students)(Total Female Students)[SEP](Program)[Cluster]
- (3) [Bar](Total Program Students Percentage)[SEP](Program) [Cluster]

From the above results, we can see that the mixed model successfully recommends the bar chart in Figure 1b as the top-1 result. Result (2) is the clustered form of the bar chart in result (1). Result (3) is also useful since it has similar meaning to the line chart in Figure 1a. The multi-type model tend to recommend what are commonly performed, thus may lack diversity (e.g., all the above results are bar charts). So one can also put single-type recommendations into the list. (We leave as a future work how to mix the results from multi-type and single-type models together for a balanced recommendation.)

When a user has chosen a specific chart type and needs auto-completion help, it is time to use single-type model for recommendations. In such scenario, our single-type models can recommend all as top-1 the area chart in Figure 1e, the bar chart in Figure 1b and the line chart in Figure 1a.

4.5 Exploring Table Representations

3039 tables (containing 20000 fields) are randomly chosen from the validation set to help visualize through t-SNE (Smilkov et al. 2016) how the embeddings generated by the shared table representation encoder work. In the left part of Figure 5, each point represents a field and the color represents its field type. In the figure, we can see the field type information is learnt by the embedding in a meaningful way. For example, date-time fields and year fields are close. One possible explanation is that they both are often used as x-axes in line charts, and thus have similar representations.

As depicted in Figure 5, the fields f_5 , f_6 and f_8 of the table in Figure 2a are marked. Three fields are close to each other, because their records are all percentages. Note that f_5 and f_6 are closer compared to f_8 because their semantics are similar (contain gender information). Some example neighbor fields (based on cosine distance) of f_8 are shown in the right part of Figure 5. We can see that all these fields are also percentages that sum up to 1, which have similar value statistics as f_8 . Please find more case study and table representation examples in appendix §F.

5 Related Work

Analysis Recommendation: For general data analysis and insight recommendation, current systems are mostly based on collaborative filtering (Marcel and Negre 2011), statistical significance (Tang et al. 2017; Ding et al. 2019), heuristic and history matching (Ehsan, Sharaf, and Chrysanthis 2016; Milo and Somech 2018), or only target for specific analysis (Zhou et al. 2020). They rarely consider the semantic meaning of table context or recommend multiple types of analysis, which are both done by Table2Charts in an end-to-end approach using large-scale human created corpus.

Chart Recommendation is one of the most important branch of analysis recommendation. Lots of visualization recommendation systems heavily rely on hand-crafted heuristics and rules, such as Voyager (Wongsuphasawat et al. 2016) and Draco (Moritz et al. 2019). Data-driven approaches are becoming popular in recent learning-based systems such as DeepEye (Luo et al. 2018), Data2Vis (Dibia and Demiralp 2019) and VizML (Hu et al. 2019). However, DracoLearn and DeepEye both learnt from low quality data and depended on hybrid with complex rule designs, Data2Vis suffered from naive end-to-end approach of character-level seq2seq generation of Vega-lite (Satyanarayan et al. 2017) JSON string, and VizML only considered design choices without handling of data queries. Please find the detailed comparison of Table2Charts with previous SOTA systems in appendix §E.4.

Structured Prediction: Filling chart templates and generating action sequences is a structured prediction problem. There are lots of related work such as NL QA (Yu et al. 2018). Table2Charts is inspired by (Gu et al. 2016; Zhou et al. 2020) to design an encoder-decoder architecture with copying mechanism as a function approximator.

Representation Learning and Pre-training: The word embedding (Bojanowski et al. 2017) and pre-training paradigm (Devlin et al. 2018) in NLP inspired us to learn pre-trained table representations for multiple tasks (Zhang and Yang 2018). The table field embedding could be useful for any down-stream data analysis tasks.

6 Conclusion

In this paper, we propose Table2Charts framework to solve single and multi-type chart recommendation tasks considering both data queries and design choices. Through copying from table fields, shared table representations are learnt to enhance performance. The proposed techniques can be widely used for data analysis tasks on tables.

References

- Bojanowski, P.; Grave, E.; Joulin, A.; and Mikolov, T. 2017. Enriching Word Vectors with Subword Information. *Trans. Assoc. Comput. Linguistics* 5: 135–146.
- Devlin, J.; Chang, M.; Lee, K.; and Toutanova, K. 2018. BERT: Pre-training of Deep Bidirectional Transformers for Language Understanding 1810.04805. URL <http://arxiv.org/abs/1810.04805>.
- Dibia, V.; and Demiralp, Ç. 2019. Data2Vis: Automatic Generation of Data Visualizations Using Sequence-to-Sequence Recurrent Neural Networks. *IEEE Computer Graphics and Applications* 39(5): 33–46.
- Ding, R.; Han, S.; Xu, Y.; Zhang, H.; and Zhang, D. 2019. QuickInsights: Quick and Automatic Discovery of Insights from Multi-Dimensional Data. In Boncz, P. A.; Manegold, S.; Ailamaki, A.; Deshpande, A.; and Kraska, T., eds., *Proceedings of the 2019 International Conference on Management of Data, SIGMOD Conference 2019, Amsterdam, The Netherlands, June 30 - July 5, 2019*, 317–332. ACM.
- Dong, H.; Liu, S.; Fu, Z.; Han, S.; and Zhang, D. 2019a. Semantic Structure Extraction for Spreadsheet Tables with a Multi-task Learning Architecture. In *Workshop on Document Intelligence (DI 2019) at NeurIPS 2019*.
- Dong, H.; Liu, S.; Han, S.; Fu, Z.; and Zhang, D. 2019b. TableSense: Spreadsheet Table Detection with Convolutional Neural Networks. In *The Thirty-Third AAAI Conference on Artificial Intelligence, AAAI 2019, The Thirty-First Innovative Applications of Artificial Intelligence Conference, IAAI 2019, The Ninth AAAI Symposium on Educational Advances in Artificial Intelligence, EAAI 2019, Honolulu, Hawaii, USA, January 27 - February 1, 2019*, 69–76. AAAI Press.
- Ehsan, H.; Sharaf, M. A.; and Chrysanthis, P. K. 2016. muVE: Efficient Multi-Objective View Recommendation for Visual Data Exploration. In *32nd IEEE International Conference on Data Engineering, ICDE 2016, Helsinki, Finland, May 16-20, 2016*, 731–742. IEEE Computer Society.
- Gu, J.; Lu, Z.; Li, H.; and Li, V. O. K. 2016. Incorporating Copying Mechanism in Sequence-to-Sequence Learning. In *Proceedings of the 54th Annual Meeting of the Association for Computational Linguistics, ACL 2016, August 7-12, 2016, Berlin, Germany, Volume 1: Long Papers*. The Association for Computer Linguistics.
- Hu, K. Z.; Bakker, M. A.; Li, S.; Kraska, T.; and Hidalgo, C. A. 2019. VizML: A Machine Learning Approach to Visualization Recommendation. In Brewster, S. A.; Fitzpatrick, G.; Cox, A. L.; and Kostakos, V., eds., *Proceedings of the 2019 CHI Conference on Human Factors in Computing Systems, CHI 2019, Glasgow, Scotland, UK, May 04-09, 2019*, 128. ACM.
- Luo, Y.; Qin, X.; Tang, N.; and Li, G. 2018. DeepEye: Towards Automatic Data Visualization. In *34th IEEE International Conference on Data Engineering, ICDE 2018, Paris, France, April 16-19, 2018*, 101–112. IEEE Computer Society.
- Macbeth, G.; Razumiejczyk, E.; and Ledesma, R. D. 2010. Cliff’s Delta Calculator: A non-parametric effect size program for two groups of observations. *Universitas Psychologica* 10(2): 545–555.
- Marcel, P.; and Negre, E. 2011. A survey of query recommendation techniques for data warehouse exploration. In Bimonte, S.; and Pinet, F., eds., *Actes des 7èmes journées francophones sur les Entrepôts de Données et l’Analyse en ligne, Clermont-Ferrand, France, EDA 2011, Juin 2011*, volume B-7 of *RNTI*, 119–134. Hermann.
- Microsoft. 2018. Open XML SDK. URL <https://github.com/OfficeDev/Open-XML-SDK>.
- Milo, T.; and Somech, A. 2018. Next-Step Suggestions for Modern Interactive Data Analysis Platforms. In Guo, Y.; and Farooq, F., eds., *Proceedings of the 24th ACM SIGKDD International Conference on Knowledge Discovery & Data Mining, KDD 2018, London, UK, August 19-23, 2018*, 576–585. ACM.
- Moritz, D.; Wang, C.; Nelson, G. L.; Lin, H.; Smith, A. M.; Howe, B.; and Heer, J. 2019. Formalizing Visualization Design Knowledge as Constraints: Actionable and Extensible Models in Draco. *IEEE Trans. Vis. Comput. Graph.* 25(1): 438–448.
- Ranzato, M.; Chopra, S.; Auli, M.; and Zaremba, W. 2016. Sequence Level Training with Recurrent Neural Networks. In Bengio, Y.; and LeCun, Y., eds., *4th International Conference on Learning Representations, ICLR 2016, San Juan, Puerto Rico, May 2-4, 2016, Conference Track Proceedings*.
- Satyanarayan, A.; Moritz, D.; Wongsuphasawat, K.; and Heer, J. 2017. Vega-Lite: A Grammar of Interactive Graphics. *IEEE Transactions on Visualization & Computer Graphics (Proc. InfoVis)* doi:10.1109/tvcg.2016.2599030.
- Smilkov, D.; Thorat, N.; Nicholson, C.; Reif, E.; Viégas, F. B.; and Wattenberg, M. 2016. Embedding Projector: Interactive Visualization and Interpretation of Embeddings URL <http://arxiv.org/abs/1611.05469>.
- Tang, B.; Han, S.; Yiu, M. L.; Ding, R.; and Zhang, D. 2017. Extracting Top-K Insights from Multi-dimensional Data. In Salihoglu, S.; Zhou, W.; Chirkova, R.; Yang, J.; and Suci, D., eds., *Proceedings of the 2017 ACM International Conference on Management of Data, SIGMOD Conference 2017, Chicago, IL, USA, May 14-19, 2017*, 1509–1524. ACM.
- Wilcoxon, F.; Katti, S.; and Wilcox, R. A. 1970. Critical values and probability levels for the Wilcoxon rank sum test and the Wilcoxon signed rank test. *Selected tables in mathematical statistics* 1: 171–259.
- Wilke, C. O. 2019. *Fundamentals of Data Visualization: a Primer on Making Informative and Compelling Figures*. O’Reilly Media.
- Williams, R. J.; and Zipser, D. 1989. A Learning Algorithm for Continually Running Fully Recurrent Neural Networks. *Neural Comput.* 1(2): 270–280.
- Wongsuphasawat, K.; Moritz, D.; Anand, A.; Mackinlay, J. D.; Howe, B.; and Heer, J. 2016. Voyager: Exploratory

Analysis via Faceted Browsing of Visualization Recommendations. *IEEE Trans. Vis. Comput. Graph.* 22(1): 649–658. doi:10.1109/TVCG.2015.2467191.

Yu, T.; Li, Z.; Zhang, Z.; Zhang, R.; and Radev, D. R. 2018. TypeSQL: Knowledge-based Type-Aware Neural Text-to-SQL Generation URL <http://arxiv.org/abs/1804.09769>.

Zhang, Y.; and Yang, Q. 2018. A Survey on Multi-Task Learning URL <http://arxiv.org/abs/1804.09769>.

Zhou, M.; Tao, W.; Ji, P.; Shi, H.; and Zhang, D. 2020. Table2Analysis: Modeling and Recommendation of Common Analysis Patterns for Multi-Dimensional Data. In *The Thirty-Fourth AAAI Conference on Artificial Intelligence, AAAI 2020, The Thirty-Second Innovative Applications of Artificial Intelligence Conference, IAAI 2020, The Tenth AAAI Symposium on Educational Advances in Artificial Intelligence, EAAI 2020, New York, NY, USA, February 7-12, 2020*, 320–328. AAAI Press.

A Charts in a Nutshell

In §2 we have briefly introduced charts and chart templates. Here, we summarize the characteristics of different chart types and illustrate our chart templates.

Definition 3. For annotation simplification, we define **x-fields** as the fields that are mapped to x-axis in line, bar, scatter and area charts, the fields mapped to legend in pie charts, and the fields mapped to curved polar axis in radar charts. We also define **y-fields** as the fields mapped to y-axis in line, bar, scatter and area charts, the fields mapped to the size of slice in pie charts, and the fields mapped to radial axis in radar charts.

For most types of charts, except for scatter chart, there can be multiple x-fields, and thus the x-axis labels become hierarchical. In such a case, each x-field represents one level. For example, if two fields named "Year" and "Month" are chosen as x-fields, x-axis labels are actually the combination of them, e.g. "2019 Jan" to "2020 Aug", forming a series of continuous months.

For most types of charts, except for scatter and pie chart, there can be multiple y-fields. Each y-field corresponds to a chart series, which is a line in line and radar chart, or a series of bars in bar chart, or an area with unique color in area chart. As a result, we can see multiple chart series in one chart, from which users can compare different series and try to find out their relationships.

- **Line Chart.** Line chart is used to show the variation trend of y-fields along the x-fields. The x-axis of line chart can be categorical, so that the records plotted along x-axis are in the index order of the field, or numerical, so that the records are in order of their values.
- **Bar Chart.** Bar chart is used for visualizing amounts (i.e. numerical values shown for some set of categories) (Wilke 2019). Bar chart supports multiple y-fields, while the layout of y-fields can either be *Clustered* or *Stacked*. The differences are:
 - *Clustered.* In this case, each bar represents the amount or value of a record in one y-field. Bars that belong to different y-fields but have the same index order in the field (e.g. the first record of each y-field) are grouped together and form a cluster.
 - *Stacked.* Different from *Clustered* manner, *Stack* manner stacks bars on top of each other within each group. Stacking is useful when the sum of the amounts represented by the individual stacked bars is itself a meaningful amount (Wilke 2019).
- **Scatter Chart.** Scatter chart is used for characterize the correlations or function relationship between x-fields and y-fields, or the trend of y-fields along x-fields. An important difference between scatter chart and other charts is that it allows the values on the x-axis to repeat. For example, the dots may form several clusters, bands or some other shapes, and that's exactly what users want to visualize. Due to its physical meaning and usage, we claim that scatter chart must have only one x-field and one y-field.

- **Pie Chart.** Pie chart is used for showing how some groups, entities, or amounts breaks down into individual pieces that each represents a proportion of the whole (Wilke 2019). Only one y-field is allowed in a pie chart because it can only visualize one value series at a time.
- **Area Chart.** Area Chart is very similar to line chart. The difference is that in area chart, the area between axis and line are commonly emphasized with colors or textures, so that the scale of color fill indicates the volumes. Commonly, area charts are used to represent accumulated totals using numbers or percentages over time².
- **Radar Chart.** The radar chart is used to compare the properties of a single component or the properties of two or more variables together³.

Chart Template Illustration. As discussed in §2.1, a chart can be abstracted as an analysis which contains two parts: selecting / referencing table fields and running specific chart creating commands / operations to organize and plot the selected fields. From all chart analysis sequence templates, we can see that the start tokens are all command tokens that indicate which type of chart it is going to construct. The following part includes two segments of field referencing tokens, separated by [SEP]. The first segment of field referencing tokens represents y-fields, while that of the second segment refer to the x-fields. (Note that, if there is no x-fields, the x-axis of the chart is indexes that start from 1.) The last token of the template is usually [SEP] which indicates the end of a chart analysis sequence. However, the last token of bar chart is <grp> which shows the how to put y-fields together.

B Details of Excel Chart Corpus

In §4.1 we briefly introduced our chart corpus. To facilitate understanding and discussion, in this section we first recap the variations in chart analysis and the basic concepts for its structural components. Then we will clarify how the raw data are processed and cleansed to form the chart corpus, with its basic statistics.

B.1 Data Cleansing

We collect and cleanup (table, charts) pairs from the raw spreadsheets using OpenXML (Microsoft 2018) library from the public web. The charts in Excel include three important ingredients: y-fields, x-fields and series names. Y-fields and x-fields are introduced and defined in §A. Series names refer to the name and meaning of each y-field, which are usually displayed in chart legend. In the paper we only focus on choosing x-fields and y-fields to fill a template, ignoring the choosing of series names. (In fact, most series names are from table headers which we use as a part of input information.)

However, due to the flexibility of spreadsheets, users can choose spreadsheet cells (a.k.a. data references) for x-fields, y-fields and series names from anywhere (e.g., from another

²https://en.wikipedia.org/wiki/Area_chart

³<https://www.pluscharts.com/why-and-when-to-use-spider-and-radar-chart/>

spreadsheet). Data of one field can be chosen from several places and concatenated together. Even worse, a user can even input the data directly instead of referencing spreadsheet cells. These will severely influence our corpus and the training of Table2Charts. So we filter out these irregular data in data cleansing.

After that, there is still a question preventing us from extracting (table, chart) pairs: Where is the source table of a chart? In spreadsheets, only the referenced cells are saved for a chart. We have to restore the whole table from which a user choose data to create the chart. In this paper, this is done by running table region and structure detection (Dong et al. 2019b,a) according to the chart data references.

In addition, a user can draw several charts of different types in one plot area in Excel spreadsheets (e.g. draw a line chart over a bar chart). These charts together are called a combo chart, while each component is called a simple chart. (Note that simple charts can still have multiple x-fields and y-fields.) In this paper, we focus on simple charts and leave combo chart recommendation as future work. Therefore, in the corpus all combo charts are split into simple charts.

Furthermore, there exists table duplication in the original spreadsheets, which leads to two main issues: 1) Too many repeated tables may mislead the real distribution, and may also confuse the model; 2) Duplicated tables may be allocated into training and testing set, leading to “data leakage” problem. To address these issues, we define **Table Schema** and do table deduplication according to it.

Definition 4 (Table Schema). Two tables are defined to have the same schema *iff* they have the same number of fields, and each field’s type (one of {String, Numerical, Date-time, Year, Unknown}) and name is correspondingly equal.

After deduplication, there are 99879 schemas in total. The schemas are sorted according to their number of tables. The distribution of the number of tables within each schema is shown in Figure 6a. We can see that only 288 schemas cover 20% of all tables, which suggests that the number of tables within each schema is very imbalanced. To mitigate this problem, we design a down sampling process. The CDF of table numbers after down sampling is also plotted in Figure 6b. We can see that the imbalance number of table problem is alleviated.

Data Cleansing Pipeline. As a summary, to cleanse the data we apply the following filters to the extracted simple charts:

1. *Data References.* If the data reference of any part (y-fields, x-fields, or series names) in a chart is invalid or separated into several parts, the chart will be dropped. Besides, we stipulate that the referenced regions of x-fields and y-fields should be in the same worksheet and aligned with each other horizontally or vertically. The chart series are further split by x-field reference to make sure that there is at most one x-field reference in one simple chart.
2. *Source Tables.* If all parts of a chart are not covered by the same source table, or the series names are not in the detected header region, or the y-field references are not in the detected value region, the chart will be dropped.

In order to validate the core effectiveness of our proposed methods, charts with hierarchical header structures are excluded in the final corpus. Empty fields and record entries are removed from the source tables.

3. *Table deduplication.* Tables are first grouped according to their schema. And within each group of tables which have the same schema, we merge tables that are exactly the same. Meanwhile, same charts (with same chart type and field references) from a table are also merged.
4. *Down Sampling.* For each schema, we first select all unique charts in it. If there are more than 10 unique tables corresponding to a unique chart, we randomly select 10 of them, otherwise we take all unique tables of the selected unique chart. After this, the unique tables that we choose is the sampled table of this schema.

Dataset Splitting. The final corpus is split into training, validation and testing set according to the table schemas in the ratio of 7:1:2. All tables and charts under the same schema will be allocated into the same set to avoid data leakage.

B.2 Corpus Statistics

In this section, some important statistics about the tables and charts of the cleaned corpus are explored.

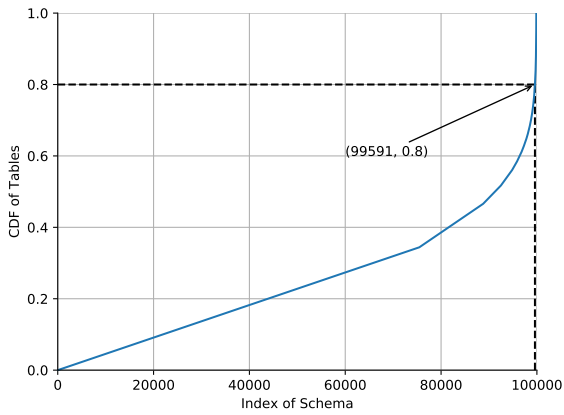
The distributions of the number of source fields and records in each table are shown in Figure 7 and Figure 8. We can see that about 99.9% tables have less than 128 fields. Thus, when training and evaluating our model, we ignore the tables which have over 128 fields and the charts generated by them. The distribution of the number of records in a table exhibit long tail characteristics, where 89.9% of tables have less than 100 records even though some tables have over thousands of records. However, we do not filter any tables according to the number of records, because no matter how many records a field has, they are finally described by the 31 data features as discussed in §D.3.

The distribution of how many charts a table generates is shown in Figure 9. From the CDF we can see that about 99.3% tables generate less than 10 charts. Although there are some tables generate over 100 charts, the amount of these tables is rather small and does not influence the balance of the separation of train/validation/test sets.

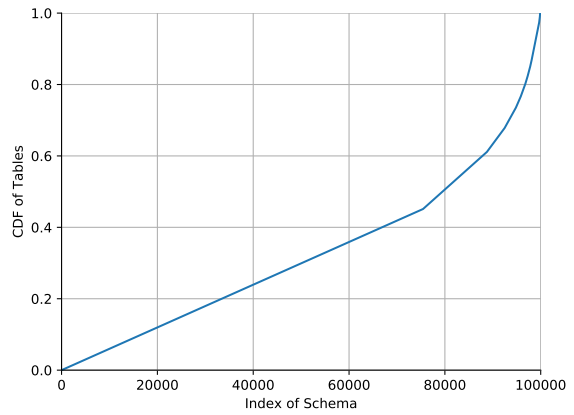
Next, we investigate the number of x-fields and y-fields in a chart. The results are shown in Figure 10. Most charts has none or only 1 x-field (99.43%); the others may contain 2 or 3 x-fields (0.54%) with hierarchical structure. For y-fields, there are about 79.60% charts having none or only 1. About 96.78% of charts have less than 5 y-fields. Thus during experiments, only the charts that have less than 5 y-fields are considered.

Then, the distribution of different chart types is shown in Figure 11. Four major chart types take about 98.91% of all charts, while two minor chart types only take the rest 1.09% of them. Consequently, the “imbalance data” problem mentioned in §1 is severe for minor chart types.

Finally, we explore the distribution of different grouping methods in bar charts, and the result is shown in Figure 12. It is worth to mention that bar charts which have only one y-field do not actually have grouping operation. In such a



(a) CDF of #Tables) Before Down Sampling.



(b) CDF of #Tables) After Down Sampling.

Figure 6: CDF of #Tables) by Schema Index Before and After Down Sampling.

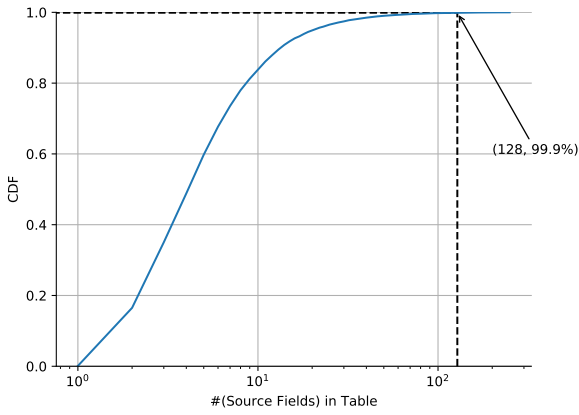


Figure 7: CDF of #Source Fields) in a Table.

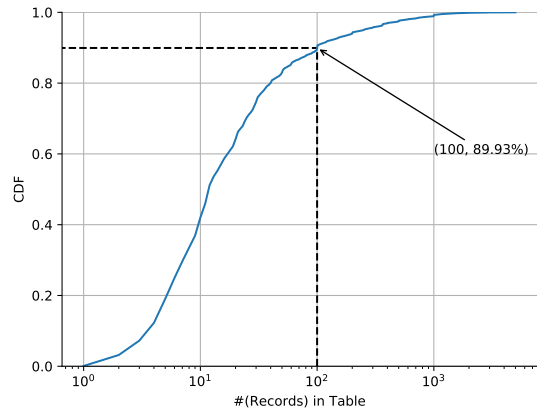


Figure 8: CDF of #Records) in a Table.

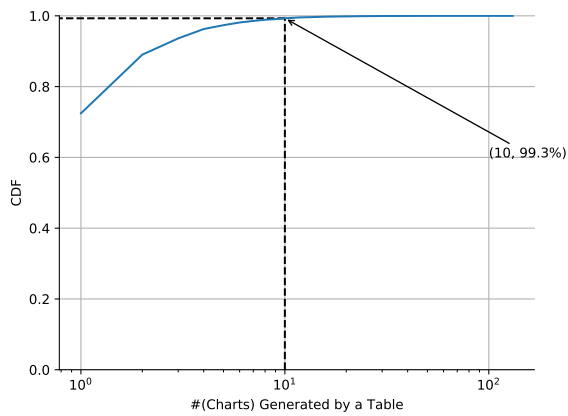


Figure 9: CDF of #Charts) Created by a Table.

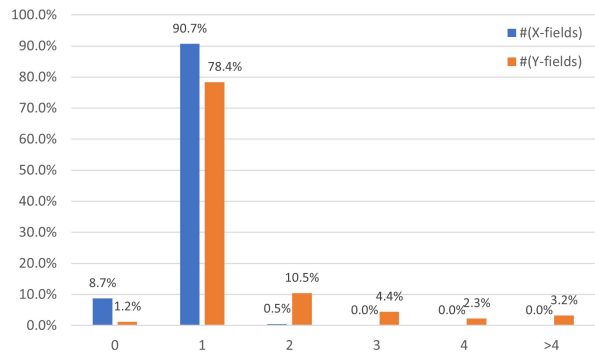


Figure 10: #X-fields) and #Y-fields) in a Chart.

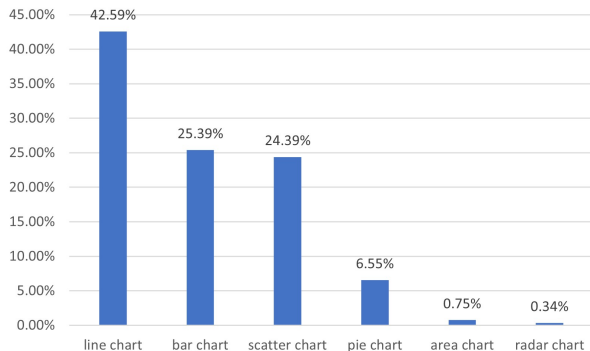


Figure 11: Distribution of Chart Types.

case, we adopt the annotation in Excel and assign the default grouping method, *clustered*, for these bar charts. From the figure, we can see that most of the bar charts adopt “Clustered” (84.20%) as their grouping methods, while the rest 15.80% bar charts takes “Stacked” as grouping methods. Therefore, as discussed in §2.1, we design the $\langle \text{grp} \rangle$ tokens for bar charts to distinguish how different value series are arranged.

C Details of Plotly Chart Corpus

To evaluate Table2Charts, Data2Viz and DeepEye fairly, we adopt public Plotly chart corpus (Hu et al. 2019) and apply the following steps to extract (table, chart) pairs.

1. *Collection and Cleaning.* Following the data processing procedure in VizML (Hu et al. 2019), we download the full corpus (205G) and adopt their data cleaning codes that remove charts without all data and duplicate charts. After cleaning, we get 475,853 (table, chart) pairs.
2. *Chart Splitting.* After cleaning, there are still two problems that prevent us from using the corpus directly. First, we only consider single charts while Plotly corpus has combo charts. Second, there is a gap of scatter chart and line chart between Plotly corpus and our definition in §A. For the former one, we split combo charts into simple charts and keep the four major chart types. For the latter one, we use chart type and mode (whether the chart draws a line) to split line chart and scatter chart according to the definition in §A.
3. *Sampling.* Lastly, we keep one of ten table pairs per user for sampling. After sampling, we get 36888 tables with 67617 charts, which contains 22644 line charts, 20053 scatter charts, 24204 bar charts and 716 pie charts.

There are two main differences in usage between Excel chart corpus and Plotly chart corpus. First, tables in Plotly only contain fields which are used for composing charts. Models don’t need to exclude fields which are not used for creating chart by users. Thus, it lowers the difficulty of data queries task (see Table 1). Second, headers of Plotly tables contain series names and axis information, e.g. “dk, y”, “fd, y”, “dk, x; fd, x; yh, x” (dk, fd, yh are series name). It makes field selection and mapping much simpler for models which

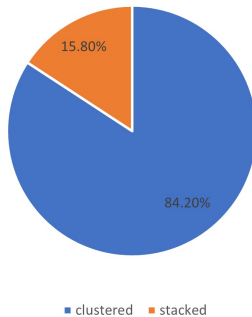


Figure 12: Distribution of Grouping Methods.

make use of header information. Therefore, for fair comparison, we remove the semantic embedding module from Table2Charts when evaluating on Plotly corpus.

D Details of Table2Charts Framework

In this section, we will dive into the details of the table-to-sequence problem formulation in §2.2 with details of the corresponding Markov decision process. Then the CopyNet DQN model which was first described in Figure 4a of §3.1 will be discussed. Also, the input token features to the input embedding network of Figure 4b will be listed for your references. Finally, we will describe the companion heuristic beam searching algorithm to the DQN.

D.1 Markov Decision Process

As described in §2.2, the Markov decision process for chart generation is based on the one for pivot table that was first defined by (Zhou et al. 2020).

Definition 5 (Chart Generation MDP). For a table \mathcal{D} , we adopt the definitions in §2.1 and §2.2 to describe the next-token chart sequence generation MDP:

- State space is $\mathcal{S}_{\mathcal{D}}^+ = \{s \mid s \in \bigcup_{l=1}^{\infty} \mathcal{A}_{\mathcal{D}}^l, s \text{ is legal}\}$, which can be viewed as a forest with chart type tokens (see §2.1) as root nodes (initial states) of the trees. $\mathcal{S}_{\mathcal{D}}^+$ contains all the prefixes of all the possible legal chart sequences that follow the chart templates.
- Action space $\mathcal{A}_{\mathcal{D}}$: The legal actions for a given state s are $\mathcal{A}_{\mathcal{D}}(s) = \{a \mid sa \in \mathcal{S}_{\mathcal{D}}^+, \forall a \in \mathcal{A}_{\mathcal{D}}\}$.
- State transition is deterministic. The transition probability from s to s' by taking action $a \in \mathcal{A}_{\mathcal{D}}(s)$ is:

$$\mathcal{P}_{\mathcal{D}}(s, a, s') = \begin{cases} 1 & \text{if } s' = sa, \\ 0 & \text{otherwise.} \end{cases}$$

- Reward function $\mathcal{R}_{\mathcal{D}}$ is designed to reflect if a user-created sequence is successfully generated:

$$\mathcal{R}_{\mathcal{D}}(s, a, s') = \begin{cases} 1 & \text{if } s' = sa \text{ and } s' \in \mathcal{G}_{\mathcal{D}}, \\ 0 & \text{otherwise.} \end{cases}$$

Here $\mathcal{G}_{\mathcal{D}}$ is a subset of $\mathcal{S}_{\mathcal{D}}^+$ which contains exactly the charts created by user for \mathcal{D} . (So $\mathcal{T}_{\mathcal{D}}^+$ is the set of all the prefixes of all the targets in $\mathcal{G}_{\mathcal{D}}$.)

- Discount rate $\gamma = 1$ so that the length of a chart sequence has no impact on its rewards.

According to Bellman optimality equation, one can easily find the optimal action-value function (the expected discounted return for the optimal policy):

$$\begin{aligned} q_*(s, a) &= \mathcal{R}_{\mathcal{D}}(s, a, sa) + \gamma \max_{a' \in \mathcal{A}_{\mathcal{D}}(sa)} q_*(sa, a') \\ &= \begin{cases} 1 & \text{if } s' = sa \text{ and } s' \in \mathcal{T}_{\mathcal{D}}^+, \\ 0 & \text{otherwise.} \end{cases} \end{aligned}$$

In other words, $q_*(s, a)$ equals to 1 if and only if sa is a prefix of a target sequence. Now as described in §2.2, the rest of the problem is to learn a good approximator for $q_*(s, a)$.

D.2 CopyNet Details

As shown in Figure 4a, there are generate (for the command tokens) and copy (for the field tokens) parts in the output of $Q(s, \mathcal{A}_{\mathcal{D}})$. The generate part contains the action value estimations for \mathcal{C} , which is a full connected layer with a binary softmax applied on the final decoder state z_T . The copy part has variable length of value estimations for $\mathcal{F}_{\mathcal{D}}$, which is a binary softmax applied on the product of z_T and a non-linear transformation of the memory $M = \{h_1, \dots, h_n\}$ (the encoder outputs). We adopt GRU in bidirectional ways for encoder RNN parts, and that in unidirectional ways for decoder parts, respectively. Thus M is simply the outputs of a bidirectional GRU for $\mathcal{F}_{\mathcal{D}} = (f_1, \dots, f_n)$. A decoder state z_t is updated by p_t from the previous state z_{t-1} in GRU cell. p_t is a linear projection from the concatenated vector of three parts: selective read vector ζ_t , context vector c_t and the token embedding $e(s_{t-1})$. Selective read vector⁴ choose the field representation from M for a field token:

$$\zeta_t = \begin{cases} h_{f_{\tau}} & f_{\tau} = s_{t-1}, \\ \vec{0} & \text{otherwise.} \end{cases}$$

Context vector is linear attention between z_{t-1} and M (where $\eta(\cdot, \cdot)$ is a linear function on two vectors):

$$c_t = \sum_{\tau=1}^n \frac{e^{\eta(z_{t-1}, h_{\tau})}}{\sum_{\tau'} e^{\eta(z_{t-1}, h_{\tau'})}} h_{\tau}.$$

The token embedding part omitted in Figure 4a is shown in Figure 4b. It is part of encoder and is shared with decoder. Three kinds of token features (see §D.3) are fused together: 1) Semantic embedding of field name (table header or database attribute string) using fastText (Bojanowski et al. 2017); 2) Categories including token type, field data type, etc.; 3) Data features about the statistics and distribution information of the field’s data value records.

The code of the whole DQN with copying mechanism can be found in the code and data supplementary materials. Please see the README.md file in the zip package for introduction to the implementation of Figure 4.

⁴Since each field token in s can only refer to one unique field from $\mathcal{F}_{\mathcal{D}}$ rather than possibly multiple source tokens in the original CopyNet, the calculation of selective read vector ζ is simplified in $Q(s, \mathcal{A}_{\mathcal{D}})$.

D.3 Token Features for Input Embedding

As shown in Figure 4b, token embedding consists of:

- Semantic embedding of field name (table header or database attribute string);
- Field categories such as data type;
- Data features about the statistics and distribution of the field’s data value records.

Semantic Embedding. Semantic embedding features are calculated from the attribute name of a field (e.g., header title of an Excel table column). In this work, we adopt fastText (Bojanowski et al. 2017) with $vocabsize = 200,000$ and $embedsize = 50$ for semantic embedding. If there are more than 1 words in the field name, the embedding of all words are averaged. We also considered BERT (Devlin et al. 2018) to calculate semantic embedding. Please see §?? for more details about our choice.

Field Categories. There are five types of categorical features which are adopted in this work.

1. *Token Types.* It shows the type of a token in an analysis sequence, which includes {PADDING, SEP, FIELD, GRP, Line, Bar, Scatter, Pie, Area, Radar}.
2. *Segment Types.* It shows to which segment a token belong in an analysis sequence. This categorical feature can be {PADDING, CAT, VAL, FIELD, GRP, OP}
3. *Field Type.* It shows the type of a field, which includes {Unknown, String, Year, DateTime, Decimal} (non-field tokens are marked as Unknown).
4. *Field Role.* It shows whether a field is in the region of counter header area of the table. The options of this categorical feature include: [InCounterHeader], [NotInCounterHeader], and [Unknown].
5. *Grouping Operation.* This categorical feature is designed for the <grp>, which can be either [Cluster], [Stack] or [Invalid].

Data features. We adopt 16 data statistics features in (Zhou et al. 2020), and design 15 new features. All 31 data features are listed in Table 3.

As shown in the 3rd and 4th columns of Table 3, all features except for *AverageLogLength* are calculated for the numeric fields while applicable ones are calculated for the string fields. Most data features are ranged in $[0, 1]$, and for those whose range may be very large, we normalized them by their 99th percentile numbers in Excel chart corpus. Data statistic features for non-field tokens remain empty (their values are assigned as zeros).

D.4 Heuristic Beam Searching

In search sampling training and beam searching inference stages of Table2Charts, we adopt a drill-down beam searching algorithm (Zhou et al. 2020). It takes the following steps to search in the action space to generate chart sequences:

1. Initially, the searching frontier only contains the sequence(s) that each consists of one specified chart type token from {[Line], [Bar], [Scatter], [Pie]}

Table 3: Data Statistic Features.

Features in (Zhou et al. 2020)	Meaning	Numeric	String	Normalized
AggrPercentFormatted	Proportion of cells having percent format	✓		
Aggr01Ranged	Proportion of values ranged in 0-1	✓		
Aggr0100Ranged	Proportion of values ranged in 0-100	✓		
AggrIntegers	Proportion of integer values	✓		
AggrNegative	Proportion of negative values	✓		
CommonPrefix	Proportion of most common prefix digit / char	✓	✓	
CommonSuffix	Proportion of most common suffix digit / char	✓	✓	
KeyEntropy	Entropy by values	✓	✓	
CharEntropy	Entropy by digits / chars	✓	✓	
ChangeRate	Proportion of different adjacent values	✓	✓	
PartialOrdered	Maximum proportion of increasing or decreasing adjacent values	✓		
Cardinality	Proportion of distinct values	✓	✓	
Spread	Cardinality divided by range	✓		
Major	Proportion of the most frequent value	✓	✓	
Benford	Distance of the first digit distribution to real-life average	✓		
OrderedConfidence	Indicator of sequentiality	✓		
New Features	Meaning	Numeric	String	Normalized
SumIn01	Summation of all values if in range [0,1]	✓		
SumIn0100	Summation of all values if in range [0,100]	✓		
Range	Values range	✓		✓
Variance	Standard deviation	✓		✓
Cov	Coefficient of variation	✓		✓
AbsoluteCardinality	Number of distinct values	✓	✓	✓
MedianLength	Median length of each record	✓	✓	✓
LengthStdDev	Standard deviation of record lengths	✓	✓	✓
AverageLogLength	Normalized string length indicating the likelihood of string values to be descriptive texts		✓	
ArithmeticProgressionConfidence	Confidence of a field to be arithmetic progression	✓		
GeometricProgressionConfidence	Confidence of a field to be geometric progression	✓		
Skewness	Skewness of numeric values	✓		
Kurtosis	Kurtosis of numeric values	✓		
Gini	Gini coefficient of numeric values	✓		
NRows	Number of rows (record entries)	✓	✓	✓

Table 4: Hyper-parameters of CopyNet Models in Different Sizes.

Model Size	Small	Medium	Large
Encoder Layers	2	2	4
Encoder Input Dim	192	320	384
Encoder Hidden Dim	128	192	224
Decoder Layers	1	1	1
Decoder Input Dim	192	256	512
Decoder Hidden Dim	128	192	256
Total Parameters	~0.8M	~1.9M	~4.9M

, [Area], [Radar]}. Chart types are chosen according to the training or inference task⁵.

2. For each round, the top-*BeamSize* scored partial / incomplete sequences in the frontier will be popped and extended as described below.
 - (a) For each state in the beam, greedily drill down (choose a with the highest $Q(s, a)$ to append) until a complete sequence is generated. The complete sequence is put into the result ranking list with $Q(s, a)$ as its score. Each non-optimal state sa ($a \in \mathcal{A}_{\mathcal{D}}(s)$) from each expansion (one calculation of $Q(s, \mathcal{A}_{\mathcal{D}})$) is put into the frontier also with $Q(s, a)$ as its score.
 - (b) No more rounds and stop searching if the number of expansions exceeds *ExpandLimit*.

As mentioned in §2.1, to restrict heuristic beam searching and eliminate some nonsense recommendations, hard constraints are defined in chart templates. For example, the data type of a y-field is forbidden to be string type. During training and inference, these hard constraints are also applied by removing illegal actions from $\mathcal{A}_{\mathcal{D}}(s)$ for each expansion in the heuristic beam searching.

The code of the above heuristic beam searching algorithm is also available in our code and data supplementary material. Please see the `README.md` file in the zip package for more details about the drill-down beam searching.

E Training and Evaluation Details

This section provide detailed setups of training and evaluations of Table2Charts and other baseline methods.

E.1 Brief Introduction to Baseline Methods

In this section, we introduce the related chart recommendation systems that exist before Table2Charts, including DeepEye (Luo et al. 2018), Data2Vis (Dibia and Demiralp 2019), DracoLearn (Moritz et al. 2019) and VizML (Hu et al. 2019). Their differences with Table2Charts are summarized in Table 5. In this paper, we run Table2Charts alongside with DeepEye and Data2Vis to compare their multi-type task performances and efficiency. While for DracoLearn and

⁵In separate training, transfer learning and single-type inference, only one chart type is used; while in mixed training and multi-type inference, four major types are all used.

VizML, we will explain in this section why they are not directly comparable with Table2Charts on the tasks.

DeepEye offline APIs (<https://github.com/Thanksyy/DeepEye-APIs>) provides two ways to determine whether a visualization is good or not and rank visualizations. One way is through expert rules, and the other way is using ML models including decision trees and LambdaMART algorithm. Both of them can provide an ordered list of visualizations when get a given table. However, DeepEye only provides public models without training scripts. Thus, we evaluate DeepEye without tuning it on our Excel chart corpus. In §4.2, only the results of DeepEye ML models are described. We find DeepEye’s ML approach works better than its rule-based one on the test set of Excel chart corpus.

Data2Vis (<https://github.com/victordibia/data2vis>) formulates the data visualization problem as an end-to-end chart generation problem. It is the only end-to-end chart recommending system we know besides Table2Charts. The model of Data2Vis is a character-level sequence-to-sequence model using RNN encoder and decoder with attention. The source sequence is a JSON string of the table data, while the target sequence is a JSON string of chart description in Vega-Lite grammar. Data2Vis model was originally trained on 4300 table-chart pairs (generated by rules then problematic instances are removed). For fair comparison, as we will describe in the next section, we re-train the Data2Vis model using the exact same Excel chart corpus used by Table2Charts. Comparing to Table2Charts, the simple character-level sequence-to-sequence model in Data2Vis is quite inefficient (very long training and inference time) than the token-level abstraction in Table2Charts. Moreover, we observe that Data2Vis frequently generate output sequences that violate the basic constraints of JSON format or reference non-existing table fields.

DracoLearn (<https://github.com/uwdata/draco>) use hard constraints and soft constraints together to restrict the design space and impose a penalty in ASP (Answer Set Programming). Meanwhile, user query can be compiled into a set of constraints, and weights of soft constrains can be learned in a RankSVM model. DracoLearn needs human defined rules as constraints and focuses on searching for charts that least violates them. This leads to very weak generative power. During empirical study we find the default behavior of DracoLearn works better on the final steps (especially design choices which are easier to formulate as constraints) of chart composing, rather than full automation of chart recommendations. Due to the space limitation, we choose not to put its results in this paper.

VizML (<https://github.com/mitmedialab/vizml>) formulate the design choices into five classification problems on visualization type, has share axis, mark type, is share x/y-axis, and is on x/y axis. The classification models used by VizML were simple fully-connected feed-forward neural networks. Part of its feature engineering work also inspired our feature design in §D.3. Unfortunately, VizML did not recommend the data queries, and cannot generate a complete chart from scratch. Thus in this paper VizML is not selected for baseline comparisons.

Table 5: Comparison between Different Chart Recommending System

System	Reco Tasks	Learning Approach	Models	Dataset	N_{data}	Data Source	Data Generation
Table2Charts	Data queries + Design Choices	End-to-end chart generation as action token sequence	CopyNet as deep Q-network	(full table, charts) pairs	197k tables with 321k charts	Web Excel files	Human
VizML	Design Choices	5 classification tasks	Fully-connected feed-forward NN	(partial table, charts) pairs	119k tables	Plotly community feed	Human
DracoLearn	Data queries + Design Choices	Soft constraints/rules weights for clingo ASP solver	RankSVM	Pairwise comparison	1100 + 10 pairs	Various	Rules → Annotations
Data2Vis	Data queries + Design Choices	End-to-end chart generation as JSON string sequence	Character level seq2seq NN	(full table, charts) pairs	11 tables with 4300 charts	Tool (Voyager)	Rules → Validations
DeepEye	Data queries + Design Choices	1. Good/bad classification 2. Ranking	1. Decision tree 2. LambdaMART	1. Good/bad chart labels 2. Pairwise comparison	42 tables with 1. 33.4k labels 2. 285k pairs	Various	Rules → Annotations

E.2 Environment Details

The experiments are run on Linux machines (or nodes) with 24 CPUs, 448 GB memory and 4 NVIDIA Tesla V100 16G-memory GPUs. As we will discuss in the next section, teacher forcing training of Table2Charts is done on 1 node, while search sampling training on 8 nodes. Data2Vis models are training on 1 node. All tests and inferences are done on 1 node with same configurations for fair comparisons.

E.3 Training Details

Training Table2Charts Some hyper-parameters of Table2Charts model are selected by conducting a series of preliminary experiments.

As shown in Figure 4b, semantic embedding of field names makes part of token embedding vectors. We try two pre-trained NLP embedding models: fastText (Bojanowski et al. 2017) with embedding size of 50 and vocabulary size of 200,000, and BERT (Devlin et al. 2018) with embedding size of 768 and vocabulary (subwords) size of 30522. Besides, we consider three different model sizes, called “small”, “medium” and “large”, with different hidden state dimensions and different number of encoder layers. The hyper-parameters are shown in Table 4.

We conduct mixed training with all combinations of embedding models and model sizes using 30 epochs of teacher forcing training, and evaluate the six models on multi-type recommendation task. Results show that compared to fastText embedding, BERT embedding increases R@1 for about 2% (from 13.07% to 14.97%), but the training time is twice of fastText. Similarly, R@1 of “small”, “medium” and “large” models are 13.07%, 13.30% and 15.37% respectively. The “large” model gains about 2% in recalls while the number of parameters is $2.5\times$ “medium” or $6.1\times$ “small” model. To make a trade-off between performance and training costs, we use fastText embedding and “medium” model size in all experiments in §4.

For all experiments in §4, each training consists of 10 epochs of teacher forcing followed by 10 epochs of search sampling. The training/validation curves of the experiments indicate that the models improve small after epoch 10. All experiments for three times and by default so that all evaluation metrics reported are averaged over three results. Due to GPU memory limitations, for all experiments the batch size is set to 512.

In our experiments, the beam searching hyper-parameters ($BeamSize$, $ExpandLimit$) are fixed to (4, 100). For neural network tuning, we use Adam optimizer with $learning_rate = 1e-4$, $\beta_1 = 0.9$, $\beta_2 = 0.999$, $\epsilon = 1e-08$, and $weight_decay = 0.01$.

For Table2Charts, teacher forcing training was done on 1 node and takes 0.1 to 1 hours according to the number of samples used in training, while search sampling training was done on 8 nodes and takes 0.1 to 8 hours. To further increase the parallelism, we apply distributed data parallel on the 4 GPUs of each node. Thus, there are 4 parallel processes in teacher forcing training and 32 in search sampling training. During the back propagation at each step, gradients from each process are averaged.

Training Data2Vis In our experiments, the sequence-to-sequence model contains a 1-layer bidirectional LSTM encoder with hidden dimension 256, and a 2-layer LSTM decoder with hidden dimension 128. We chose these hyper-parameters (number of layers and hidden dimension) to make the parameter size of the model (~1.94M) comparable to the parameter size of Table2Charts (~1.9M).

Following Data2Vis, the source sequence is one row randomly sampled from the table, and we encode the source sequence by a list of field-value pairs. For target sequence, While Data2Vis uses Vega-Lite grammar to encode a chart, we encode a chart with a chart template (see §2.1 for details), a set of attribute-value pairs for simplification. The attributes of a chart include x , y , $type$, $group$, where $group$ only exists for bar chart. A set of transformations are performed on the source and target sequence as Data2Vis does. In the source and the target sequences, the string and numeric field names are replaced with shortened notations “str” and “num”. Here is an example: $source$: `[["str0", "Use of ICT"], ["num0", "1.27"], ["num1", "1.62"]]`, $target$: `[{"type": "bar", "x": ["str0"], "y": ["num0", "num1"], "group": "clustered"}]`. To generate one table-chart pair for the training set, the table is randomly sampled twice to generate two training samples, resulting in 470486 training pairs in total.

Following the training configurations of Data2Vis, in our experiments, the model uses a fixed learning rate of 0.0001 with an Adam optimizer. According to our Excel dataset, 98% of the source sequences have fewer than 471 characters,

while 99% target sequences have fewer than 130 characters. Therefore, the maximum source length and target length are set to 500 and 130. The vocabulary sizes of source and target are 98 and 42. The model is trained for nearly 30000 steps, with a batch size of 16.

For Data2Vis, the training time is much longer than Table2Charts since its character-level NN leads to very long sequences. On 1 node, its training time will be 8 to 12 hours with 4 GPUs.

E.4 Evaluation Details

In this section, we elaborate the evaluation details on data queries, design choices and overall chart recommendation tasks, and how evaluation metrics, *i.e.*, recall at top- k , are calculated for each task.

Data queries only focus on field selection when composing a chart. Given a table, if the field set of a recommended chart in the top- k ranked list matches any of user-created charts of the table, this recommended chart is considered to be successfully recalled *w.r.t.* data queries. Thus, recall at top- k of data queries is calculated as

$$R@k = \frac{\#(\text{Tables Successfully Recalled})}{\#(\text{Tables})}. \quad (1)$$

Design choices in this paper include field mapping (*i.e.*, map the selected fields into x-axis and y-axis of a chart), chart type choosing and grouping operation choosing (*i.e.*, whether stacked or clustered, only for bar chart). To evaluate design choices, we consider the chart patterns (*i.e.*, the x- and y-field combinations of a chart) of user created charts for one table. A chart pattern is considered to be recalled if it appears in the top- k recommended chart list. Thus, the recall rate is calculated as the following:

$$R@k = \frac{\#(\text{Charts Patterns Successfully Recalled})}{\#(\text{Charts Patterns})}, \quad (2)$$

where the denominator is the total number of chart patterns, and the numerator is the number of chart patterns that shows up in the top- k filtered ranked list of the table.

The overall chart recommendation task combines data queries and design choices tasks. The calculation of recall *w.r.t.* the overall task is also Eq. 1, while the “table successfully recalled” means at least one chart in the top- k recommendations completely matches a user-created chart.

Remarks on Evaluations of DeepEye. The grouping operation of bar chart is not considered in DeepEye, since it does not distinguish these two grouping operations.

Remarks on Evaluations of Data2Vis. *BeamSize* is set to 15 for data query and overall chart recommendation, and set to 30 for design choices.

Remarks on Evaluations of Table2Charts. *BeamSize* is set to 4 and *ExpandLimit* is 100, which are the same as in search sampling training.

E.5 Human Evaluation

The human evaluation is conducted on 80 common HTML tables crawled from the public web. The 80 tables belong to 71 schemas. For each table, the top-1 recommended

Table 6: The Rating Distribution of Recommended Charts

Rating	1	2	3	4	5	Avg	≥ 4	≥ 3	≤ 2
Table2Charts	24	29	21	33	55	3.41	88	109	53
Data2Vis	27	32	29	34	40	3.17	22	54	108
DeepEye	72	36	32	20	2	2.04	74	103	59

chart from the three recommendation systems, *i.e.* DeepEye, Data2Vis and Table2Charts, are evaluated by 3 different experts randomly chosen from all the 5 experts.

A chart is rated by an integer score from 1 to 5 (higher score indicates better chart), and the criteria mainly focus on the following aspects: (1) if the chart is meaningful with respect to the table; (2) if the appropriate table columns are selected; (3) if the appropriate chart type is adopted; (4) if the chosen columns are mapped to the right axis (x or y). Additionally, whether a table is unsuitable for generating any chart is reported.

After filtering out the tables reported to be unsuitable for generating a chart by at least one expert, there are 54 tables left, belonging to 49 schemas. The distribution of the rating on these tables is shown in Table 6. It demonstrates that Table2Charts has the highest average score, and the amount of good charts (rating=5, rating ≥ 4 , rating ≥ 3) is the largest, while the amount of bad charts (rating ≤ 2) is the smallest.

To compare Table2Charts with Data2Vis and DeepEye respectively, we conducted Wilcoxon signed-rank test and computed Cliff’s delta effect size. The Wilcoxon signed-rank test is a non-parametric statistical hypothesis test used to compare two related samples whether their population mean ranks differ. Cliff’s delta effect size measures how often the values in one distribution are larger than the values in another distribution. The comparison of two models are based on two lists of mean ratings over schemas, where the elements in the two lists are paired (because the corresponding ratings are for the same schema), satisfying the prerequisite of Wilcoxon signed-rank test. Human evaluation result shows that Table2Charts performs better than DeepEye and Data2Vis, see §4.2 for more details.

The human evaluated tables and the ratings on charts are provided in the code and data supplementary materials. Please see the README.md file in the zip package for more details on the human evaluation study.

F Empirical Studies

In this section, we use more examples to validate the results of Table2Charts framework, and elaborate more insights of shared table representations.

F.1 Chart Recommendation Case Studies

We first test Table2Charts framework with 3 example tables in Figure 13, Figure 14 and Figure 15 to validate the effectiveness of the proposed method. For each table, we report the chart analysis sequences that originally generated by users (**Original**), top-5 recommended chart analysis given by multi-type model (**Multi-Type Reco**), and top-1 recommendations of each chart type according to the corresponding single-type model (**Single-Type Reco**). For each recom-

	Percent of Responses:	Good	Very Good	Excellent	% Excellent Target	ON % Positive Avg	% Positive
Oct-Dec 2014 (n=179)		2.8	24.0	73.2	72.0	98.6	100.0
Jan-Mar 2015 (n=192)		2.6	25.5	70.8	72.0	98.7	99.8
Apr-Jun 2015 (n=189)		3.2	20.0	75.1	72.0	98.8	98.4
Jul-Sep 2015 (n=171)		3.5	26.3	70.2	72.0	98.8	100.0

Figure 13: Example Table 1.

Table 7: Original and Recommended Chart of Example Table 1.

	Chart	Score
Original	[Line] (% Excellent Target)(ON % Positive Avg)(% Positive) [SEP] (Percent of Response) [SEP] [Bar] (Good)(Very Good)(Excellent) [SEP] (Percent of Response) [Stack]	- -
Multi-Type Reco	[Bar] (Good)(Very Good)(Excellent) [SEP] (Percent of Response) [Stack]	0.996
	[Line] (% Excellent Target)(ON % Positive Avg)(% Positive) [SEP] (Percent of Response) [SEP]	0.995
	[Line] (% Excellent Target)(ON % Positive Avg)(% Positive) [SEP] [SEP]	0.121
	[Line] (% Positive)(% Excellent Target) [SEP] (Percent of Response) [SEP]	0.03
	[Line] (ON % Positive Avg)(% Excellent Target) [SEP] (Percent of Response) [SEP]	0.03
Line Reco	[Line] (% Excellent Target)(ON % Positive Avg)(% Positive) [SEP] (Percent of Response) [SEP]	0.995
Bar Reco	[Bar] (Good)(Very Good)(Excellent) [SEP] (Percent of Response) [Stack]	0.996
Scatter Reco	[Scatter] (Good) [SEP] (Excellent) [SEP]	0.0001
Pie Reco	[Pie] (Good) [SEP] [SEP]	0.0004
Area Reco	[Area] (% Excellent Target)(ON % Positive Avg)(% Positive) [SEP] (Percent of Response) [SEP]	0.794
Radar Reco	[Radar] (% Excellent Target)(ON % Positive Avg)(% Positive) [SEP] (Percent of Response) [SEP]	0.582

		Volatility of the exchange rate (lhs)	Volatility of stock market (lhs)	Spread between BEONIA and key policy rate (lhs)	Spread between bond yields and key policy rate (lhs)	Real GDP growth rate (rhs)	FSIX (lhs)
2006	I	-0.99362	-0.58128	-4.24348	-1.32873	-7.14711	7.093183
	II	-0.4759	-0.39348	-2.99567	-1.15894	-5.02399	4.898093
	III	6.58E-02	0.562761	-1.9901	-0.80608	-2.1676	3.30633
	IV	0.520683	-0.0276	0.734996	-0.41735	0.810692	4.651887
...
2016	I	-0.79631	-0.66146	-0.16075	0.212734	-1.40579	3.859553
	II	-0.91892	-0.95515	-0.14545	0.280418	-1.73911	2.049268
	III	-1.19545	-0.79933	7.17E-02	0.219766	-1.70333	2.831469
	IV	-1.11139	-0.28892	7.46E-02	0.219766	-1.10591	2.466321

Figure 14: Example Table 2.

Table 8: Original and Recommended Chart of Example Table 2.

	Chart	Score
Original	[Line] (Real GDP growth rate (rhs)) [SEP] (EMPTY[0]) ⁶ (EMPTY[1]) [SEP]	-
	[Line] (FSIX (lhs)) [SEP] (EMPTY[0])(EMPTY[1]) [SEP]	-
	[Bar] (Volatility of the exchange rate (lhs))(Volatility of stock market (lhs))(Spread between BEONIA and key policy rate (lhs)) (Spread between bond yields and key policy rate (lhs)) [SEP] (EMPTY[0])(EMPTY[1]) [Stack]	-
Multi-Type Reco	[Bar] (Volatility of the exchange rate (lhs))(Volatility of stock market (lhs))(Spread between BEONIA and key policy rate (lhs)) (Spread between bond yields and key policy rate (lhs)) [SEP] (EMPTY[0])(EMPTY[1]) [Stack]	0.954
	[Bar] (Volatility of stock market (lhs))(Spread between BEONIA and key policy rate (lhs)) (Spread between bond yields and key policy rate (lhs)) [SEP] (EMPTY[0])(EMPTY[1]) [Stack]	0.782
	[Line] (FSIX (lhs)) [SEP] (EMPTY[0])(EMPTY[1]) [SEP]	0.190
	[Bar] (Volatility of the exchange rate (lhs))(Volatility of stock market (lhs))(Spread between BEONIA and key policy rate (lhs)) (Spread between bond yields and key policy rate (lhs)) [SEP] (EMPTY[0]) [Stack]	0.064
	[Bar] (Volatility of stock market (lhs))(Spread between BEONIA and key policy rate (lhs)) (Spread between bond yields and key policy rate (lhs)) [SEP] (EMPTY[0]) [Stack]	0.044
Line Reco	[Line] (Real GDP growth rate (rhs)) [SEP] (EMPTY[0])(EMPTY[1]) [SEP]	0.250
Bar Reco	[Bar] (Volatility of the exchange rate (lhs))(Volatility of stock market (lhs))(Spread between BEONIA and key policy rate (lhs)) (Spread between bond yields and key policy rate (lhs)) [SEP] (EMPTY[0])(EMPTY[1]) [Stack]	0.954
Scatter Reco	[Scatter] (Real GDP growth rate (rhs)) [SEP] (EMPTY[0])	0.002
Pie Reco	[Pie] (FSIX (lhs)) [SEP] (EMPTY[0])(EMPTY[1]) [SEP]	0.001
Area Reco	[Area] (Volatility of the exchange rate (lhs))(Volatility of stock market (lhs))(Spread between BEONIA and key policy rate (lhs)) (Spread between bond yields and key policy rate (lhs)) [SEP] (EMPTY[0])(EMPTY[1]) [SEP]	0.622
Radar Reco	[Radar] (Volatility of the exchange rate (lhs))(Volatility of stock market (lhs))(Spread between BEONIA and key policy rate (lhs)) (Spread between bond yields and key policy rate (lhs)) [SEP] (EMPTY[0])(EMPTY[1]) [SEP]	0.716

Name	15-Mar	22-Mar	29-Mar	5-Apr	12-Apr	19-Apr	26-Apr	Total	% of Total
Alice	760	930	1060	980	1260	1050	1050	7090	26.42%
Bob	820	360	870	930	810	1050	660	5500	20.50%
Clark	200	615	500	550	940	390	540	3735	13.92%
David	535	0	695	875	1110	1020	1005	5240	19.53%
Eme	620	220	980	780	690	840	1140	5270	19.64%

Figure 15: Example Table 3.

Table 9: Original and Recommended Chart of Example Table 3.

	Chart	Score
Original	[Bar] (Total Time) [SEP] (Name) [Cluster]	-
	[Pie] (% of Total) [SEP] (Name) [SEP]	-
Multi-Type Reco	[Bar] (Total Time) [SEP] (Name) [Cluster]	0.748
	[Bar] (% of Total) [SEP] (Name) [Cluster]	0.624
	[Pie] (Total Time) [SEP] (Name) [SEP]	0.079
	[Bar] (% of Total) [SEP] [SEP]	0.061
	[Pie] (% of Total) [SEP] (Name) [SEP]	0.052
Line Reco	[Line] (% of Total) [SEP] (Name) [SEP]	0.995
Bar Reco	[Bar] (Total Time) [SEP] (Name) [Cluster]	0.999
Scatter Reco	[Scatter] (% of Total) [SEP] [SEP]	0.843
Pie Reco	[Pie] (% of Total) [SEP] (Name) [SEP]	0.984
Area Reco	[Area] (Total Time) [SEP] (Name) [SEP]	0.988
Radar Reco	[Radar] (% of Total) [SEP] (Name) [SEP]	0.990

mended chart, we also report the score (in range [0, 1]) given by the model. The results are summarized in Table 7, Table 8 and Table 9.

From these results of examples, we can show that our multi-type model can recommend the charts that originally created by user within top-5 recommendations. For example table 1, our model can distinguish the f_2-f_4 as a group and f_5-f_7 as a group. With the first three fields that are showing the level of an item or attribute, our multi-type model recommend stacked-bar chart to present the relationship of the three fields. While the last three fields do not have relationship with each other and they are more likely in a parallel sense, our model recommend line chart to present how these fields change along with the first field. Besides, the single-type model for area chart also recommend an area chart with high score. The field selection of area chart is the same as the recommended line chart. This is because area chart can be viewed as the line chart with color filled below the plot line. In this sense, the recommended area chart is appropriate.

For the second example table, the first two columns do not have header. However, Table2Charts can recognize them as year and quarter, and select both of them as x-axis (multi-level category). One of user-created line chart and bar chart show up in the recommendation of multi-type model with high score, while the other user-created line chart is recommended as the top-1 in line-chart model recommendation. In addition, we can also observe that the top-1 recommendation of area chart model and radar chart model also have high score. These two recommended charts are also reasonable because the area chart can be viewed as a continuous version of the bar chart, while the radar chart as circle version of the bar chart.

the multi-type model can distinguish two pairs of (Lower bound (95%)) and (Upper bound (95%)), and create line chart with them separately. One possible explanation is that through copy mechanism, the neighbor fields are more likely to be selected as category or values together.

For the third example table, the last two fields have rather similar meanings. (% of Total) is the unified field of (Total Time). The recommended charts by multi-type model main select these two fields and design bar and pie charts. Note that the single type recommendation of pie chart use (% of Total) as value while that of bar chart use (Total Time). This is more reasonable because bar chart can show the absolute value along y-axis and pie chart is naturally suitable for unified fields. Furthermore, the single-type model for area chart and radar chart also recommend two corresponding chart with high score. The area chart is similar to the top-1 bar chart if we replace each bar with continuous area. Therefore, it can be regarded as a good choice. As for the recommended radar chart, it is also reasonable because it can also show the values (percentages) of each person. This example validate that our single-type model can give more diverse results.

F.2 T-SNE Insights on Table Representations

In this section, we elaborate more details on visualization of shared table representations with t-SNE, where fields with similar embedding vectors are close to each other. The perplexity and learning rate for t-SNE is first set to 20 and 10 for

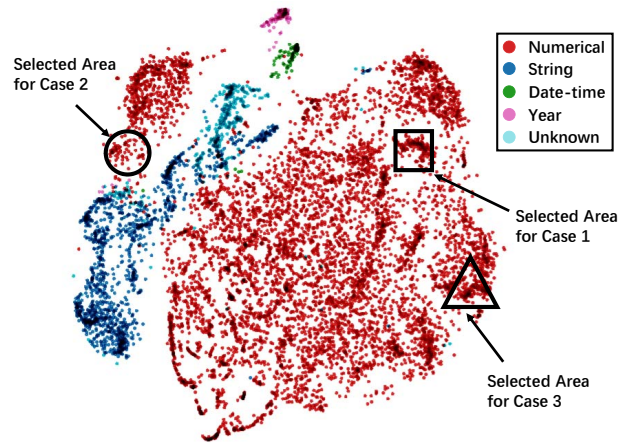


Figure 16: T-SNE Result and the Three Selected Cases.

the first 50 iterations, and then they are set to 80 and 0.1 for the rest 150 iterations. The visualization results are shown in Figure 5. In the following, we present three local details of the t-SNE result to validate that Table2Charts framework can learn meaningful shared table representations.

- **Case 1.** We choose four fields that are located in the squared area in Figure 16, and show them (highlight in red) with their tables in Figure 17. We can see that four selected fields all have headers that represent a country. They are all the second field of the table. The records of the fields are all numerical values, which shows how some attributes of a country change along year.

- **Case 2.** Next, we choose four fields that are located in the circular area in Figure 16, and show them (highlight in red) with their tables in Figure 18. The selected four fields are all index that are the first fields of the table. Although they all have the numerical records, but the numbers lose the numerical property (they should not be used for mathematical operation). Their roles are the indicator of each record. Thus, these fields are close to string fields cloud in Figure 16 (dark blue points).

- **Case 3.** Finally, we choose four fields that are located in the triangular area in Figure 16, and show them (highlight in red) with their tables in Figure 19. These fields are all correlated with currency and money. They all have clear signals of “\$” or “Dollar” in the header or records. The embedding vectors of these fields are similar, and thus, they form cluster in the results of t-SNE.

NAICS Industry Title	U.S.	State	San Juan
2001	0.0%	-0.4%	2.7%
2002	-1.1%	-1.5%	-1.1%
...
2015	2.1%	2.9%	1.7%
2016	1.7%	3.1%	2.2%

Example - 1

	Japan	United States	Euro Area
2000	143.8	-	67.9
2001	153.6	53.0	66.7
...
2019	251.9	106.4	87.6
2020	251.8	106.1	85.5

Example - 2

	England	London
1997	3.57	3.93
1998	3.57	4.25
...
2009	6.28	8.04
2010	6.69	8.96

Example - 3

Year	Scotland	England	Wales	Northern Ireland
1990	15.3	3.7	0.7	1.6
1991	14.0	4.5	0.5	1.2
...
2010	2.7	2.3	0.2	0.2
2011	5.1	2.5	0.3	0.3

Example - 4

Figure 17: Example Fields and Tables for Case-1.

Course Code	Course Name	...	Extra Funding	Total Funding
10	English	...	-	£1,350.00
11	Maths	...	£1,000.00	£1,750.00
...
17	Excel	...	-	£0.00
18	Database	...	-	£0.00

Example - 1

VerminID	Name	...	Sum Of Poison Lbs	# bugs killed
44	Wasp	...	7	1050
52	BedBug	...	58	8700
...
199	Mouse	...	227	6810
352	Bear	...	7	0.7

Example - 2

Index	Bill Impact Frequency Range (%)	...	RH3 Cumulative Bill Impacts
1	Less than 5	...	0%
2	5% to 10%	...	1%
...
17	80% to 85%	...	100%
18	Greater than 85%	...	100%

Example - 3

category	Birth order	...	SBA	% POP
1	1	...	70.7	23.7
2	2-3	...	60.6	38.1
3	4-5	...	53.8	22.7
4	6+	...	42.6	15.6

Example - 4

Figure 18: Example Fields and Tables for Case-2.

	Costs	Sales
Oct	\$37,500	\$750,000
Nov	43,125	791,300
Dec	49,175	830,900
...
Feb	63,900	881,400
Mar	72,850	885,800

Example - 1

Month	Marketing Expenditure (\$ '000)	Sales (\$ '000)
Jul-08	300	530
Aug-08	346	635
...
May-10	682	835
Jun-10	234	352

Example - 2

month	customers	revenue
January	5	\$1,100.00
February	12	\$1,200.00
...
June	45	\$8,500.00
July	40	\$7,500.00

Example - 3

Year	GDP in billions of current dollars	GDP in billions of chained 2000 dollars
1980	2,789.5	5,161.7
1981	3,128.4	5,291.7
...
2006	13,178.4	11,294.8
2007	13,807.5	11,523.9

Example - 4

Figure 19: Example Fields and Tables for Case-3.